1996

Characterizing the Degradation of Nylon-11 and PVDF in a Flexible Oil Pipe and Cure Monitoring of Chemflake Vinylester

John Chen Yang
College of William & Mary - Arts & Sciences

CHARACTERIZING THE DEGRADATION OF NYLON-11 AND PVDF IN A FLEXIBLE OIL PIPE AND CURE MONITORING OF CHEMFLAKE VINYLESTER

A Thesis

Presented to

The Faculty of the Department of Chemistry

The College of William and Mary in Virginia

In Partial Fulfillment

Of the Requirements for the Degree of

Master of Arts

---

by

John C. Yang

1996

APPROVAL SHEET

This thesis is submitted in partial fulfillment of the requirements for the degree of

Master of Arts

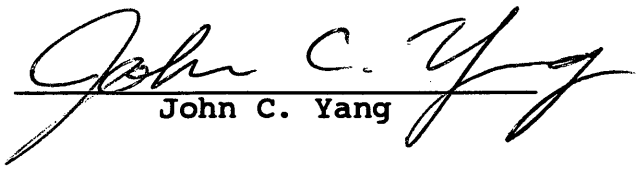

John C. Yang

Approved, July 1996

David E. Kranbuehl

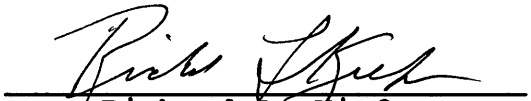

Richard L. Kiefer

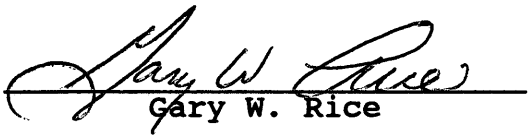

Gary W. Rice

ACKNOWLEDGEMENTS

The author would like to express his gratitude towards Dr. Kranbuehl for his guidance, without which none of this thesis could have been written. Also the writer wishes to thank all the undergraduate students involved in this project, especially Eric Chu, Andree Ebersole, Whitney Erwin, Nicole Haralampus, and Paul Haase. In addition, this project would not have gotten this far without the dedication of Dr. David Hood and Wendy Newby. Lastly, the author is grateful to Dr. Kiefer and Dr. Rice for their critique of this final draft.

Table of Contents

	Page
Acknowledgements	iii
List of Figures	v
List of Tables	vii
Abstract	viii
Chapter 1. Introduction	2
Chapter 2. Chemistry of Nylon-11, PVDF, and Chemflake	8
Chapter 3. Experimental Techniques	25
Chapter 4. Experimental Setup and Results	55
Chapter 5. Conclusions	98
Bibliography	101
Vita	104

List of Figures

Figure		Page
1.1	Design of Flexible Oil Pipe	6
2.1	Rotary and Offshore Drilling Rigs	20
2.2	Crystallites within Bundled Lamellae	10
2.3	Acid-Catalyzed Hydrolysis of Amide Bond	22
3.1	Impedance Measurement Sensor	26
3.2	Parallel Plate Capacitor	27
3.3	Polarization Mechanisms	30
3.4	Effect of Dielectric Materials in Capacitor	33
3.5	Fluid Flow Representation	38
3.6	Viscometers	39
3.7	DSC System	44
3.8	Ideal DSC Scan	44
3.9	Barcol Hardness Tester	46
3.10	Operation of Tensile Machine	48
3.11	Schematic of Tensile Test Sample	49
3.12	Stress-Strain Diagram	50
4.1	FDEMS Nylon in 95°C 95% IRM/5% H_2O - ϵ'	67
4.2	FDEMS Nylon in 95°C 95% IRM/5% H_2O - ϵ'' x ω	67
4.3	MW vs. Days Nylon 105°C at various pHs	71
4.4	Log MW vs. Days Nylon 105°C at various pHs	71
4.5	MW vs. Days Nylon 105°C various H_2O cuts	72
4.6	Log MW vs. Days Nylon 105°C various H_2O cuts	72
4.7	Ln MW vs. Days Nylon five temperatures	73
4.8	Ln k vs. 1/T Nylon Arrhenius Fit	73
4.9	MW vs. Days Wellstream PVDF in various cond.	76
4.10	Log MW vs Days WS PVDF in various cond.	76
4.11	MW vs. Days Coflexip PVDF in various cond.	77
4.12	Log MW vs Days Coflexip PVDF in various cond.	77
4.13	FDEMS PVDF in 130°C Aniline - Wellstream	78
4.14	FDEMS PVDF in 130°C Aniline - Coflexip	78
4.15	FDEMS PVDF in Glycol/TEAC - Wellstream	79
4.16	FDEMS PVDF in Glycol/TEAC - Coflexip	79
4.17	ϵ'' vs Days PVDF in Aniline	80
4.18	ϵ'' vs Days PVDF in EG/10% TEAC	80
4.19	Wt Loss PVDF in various cond. - Wellstream	82

4.20	Wt Loss PVDF in various cond. - Coflexip	82
4.21	FDEMS PVDF in 130°C air - Wellstream	83
4.22	FDEMS PVDF in 130°C air - Coflexip	83
4.23	FDEMS PVDF in 130°C 95% IRM/5% H_2O - WS right	84
4.24	FDEMS PVDF in 130°C 95% IRM/5% H_2O - WS left	84
4.25	Wt Loss PVDF in 130°C 95% IRM/5% H_2O	85
4.26	FDEMS deplasticized PVDF in 95% IRM/5% H_2O	86
4.27	DSC Chemflake time 0 hours	87
4.28	DSC Chemflake time 1 hour	87
4.29	DSC Chemflake time 2 hours	88
4.30	DSC Chemflake time 4 hours	88
4.31	DSC Chemflake time 8 hours	89
4.32	DSC Chemflake time 24 hours	89
4.33	DSC Chemflake time 48 hours	90
4.34	FDEMS data and Degree of Cure of Chemflake	92
4.35	FDEMS vs Alpha during cure of Chemflake	92
4.36	FDEMS data and Barcol Hardness of Chemflake	93
4.37	FDEMS vs Hardness during cure of Chemflake	93
4.38	FDEMS Chemflake in 45°C HCl - in Vapor	94
4.39	FDEMS Chemflake in 45°C HCl - in Liquid	94
4.40	Wt Change Chemflake in 45°C HCl	96
4.41	Hardness Change Chemflake in 45°C HCl	96

List of Tables

Table		Page
2.1	Properties of various types of Nylon	21
4.1	Nylon-11 Testing environments	68
4.2	MWs of Nylon-11 in various 105°C conditions	69
4.3	MWs of Nylon-11 in other temp. conditions	70
4.4	PVDF Testing environments	74
4.5	MWs of PVDF in various 130°C conditions	75
4.6	Wt change of Wellstream PVDF in various cond.	81
4.7	Wt change of Coflexip PVDF in various cond.	81
4.8	ΔH_{rxn} during cure of Chemflake	91
4.9	Barcol-Hardness during cure of Chemflake	91
4.10	Wt change of Chemflake in 45°C HCl	95

Abstract

This study examines the accelerated aging of polymer materials with the aid of various testing methods. The first part focuses on composite systems used in the oil industry by examining the bulk property of these plastics. Both nylon-11 (Rilsan) and poly(vinylidene fluoride) (PVDF) have played an important role on the oil platforms in the North Sea. The kinetic rate of hydrolysis of nylon-11 is seen through the study of its temperature and pH dependence at various percentages of water, which is important in determining the degree of degradation at various positions of the nylon-11 being used in the pipe construction. PVDF provides a higher temperature inner fluid barrier in the oil pipe, and its stability is observed by similarly testing its microscopic and macroscopic degradation properties during immersion in various harsh chemical environments.

The second part of this study examines the cure and degradation processes of a vinylester coating, Chemflake, that is used in protecting steel tanks from acidic conditions. Using *in situ* frequency dependent electromagnetic sensing (FDEMS), the ionic mobility and

the behavior of pendant polar groups of the polymeric backbone are studied qualitatively. Hardness measurements along with degree of cure correlate well with the FDEMS sensor data and show empirically the degradation of this coating in a highly acidic environment at elevated temperature.

CHARACTERIZING THE DEGRADATION OF NYLON-11 AND PVDF IN A FLEXIBLE OIL PIPE AND CURE MONITORING OF CHEMFLAKE VINYL ESTER

CHAPTER 1. Introduction

The focus of the first part of this study is to understand and characterize the degradation of Rilsan and PVDF in an aging environment. Through interpretation with the data from the accelerated control-study in the lab, continuous *in situ* field data can provide a wealth of information regarding the integrity of the pipe. With the development of more advanced frequency dependent electromagnetic sensing (FDEMS) techniques, the remote monitoring of polymeric oil pipes will prove to be critical not only in saving frequent unnecessary replacement costs, but also predicting and preventing premature pipe failure.

In the late 1960's, sizeable oil reserves were discovered beneath the North Sea. Claims were rapidly made and to this date, those countries bordering this body of water have divided the territory for its rich resource. Unfortunately, the North Sea is plagued by a volatile weather pattern. During the winter months, storms are

especially violent and therefore most of the drilling and repair are performed over the summer months.

Permanent oil platforms produce a tremendous amount of cash flow. However, the high cost of initial setup and daily maintenance as well as the risk of sudden failure ensure that no one individual group own more than a quarter of the platform.[1]

In addition to the bad weather and high start-up cost, the presence of strict environmental regulations has made the development of monitoring techniques of a flexible off-shore pipe consisting of nylon-11 or PVDF (see **Fig. 1.1**) a necessity. This advanced pipe construction enables the entire structure to withstand high internal temperature and fluid friction as well as the lower water temperature in the external environment due to the properties of the polymers, all at depths of several thousand meters.[2]

Degradation is inevitable in all types of polymer, including Nylon-11 and PVDF, but the rate varies according to the material and its surroundings. The aging study in the laboratory attempts to simulate operating conditions and is accelerated through the use of higher temperatures and more severe chemical environments. The aging study of

Nylon-11 has been monitored extensively in this lab for the past few years (see **ref. 1, 3, and 4**) and is close to its last phase. Work on PVDF recently began and is not expected to be complete within the next year.

Since nylon-11 is exposed to variable oil-water environments, testing of this polymer involves the use of different water-to-oil ratios at temperatures between 70°C and 120°C. The use of a proper range of buffer systems is also critical since polyamides are highly susceptible to acid-catalyzed degradation.

PVDF, being a higher temperature inner-layer fluid barrier which does not hydrolyze under acidic conditions, is currently undergoing tests in high temperature environments resembling the treatment of the pipe with chemicals. These chemicals include quaternary amines in ethylene glycol for corrosion inhibition, ether and phosphonate mixtures for scale prevention, and ammonium bisulfate solutions to promote oxygen scavenging. In addition, an earlier study (late 1995) of PVDF from two different suppliers (Solvay-Wellstream and Atochem-Coflexip) involves four conditions: continuous aging of the PVDF at 130°C, in aniline at 130°C, in 10% tetraethylammonium chloride/ethylene glycol at 130°C, and

in an acidic oil-water environment.

The second part of this study looks at the cure and degradation of Chemflake by using FDEMS coupled with various physical measurements. Chemflake is a glass-flake reinforced vinyl ester coating used and provided by the Norsk Hydro Research Center in Porsgunn, Norway, for coating steel tanks used to store large quantities of HCl for the synthesis of polyvinyl chloride. After it is cured, it needs to be tested to withstand the penetration of chlorine to a high degree. An understanding of the curing process of Chemflake will provide a good insight into differences between various mixture batches as well as the extent of cure prior to use. In addition, it is also important to understand the rate of degradation seen in the material after long-term exposure to HCl. An apparatus is set up for this testing purpose with the acid bath regulated to a temperature of 45°C.

It is the hope of this study to understand and interpret the significance and correlation of laboratory dielectric measurements with bulk physical tests. Though this study encompasses a variety of polymers and composites, an overall understanding of cure monitoring and degradation process is sought using FDEMS.

Figure 1.1 Design of flexible oil pipe[5]

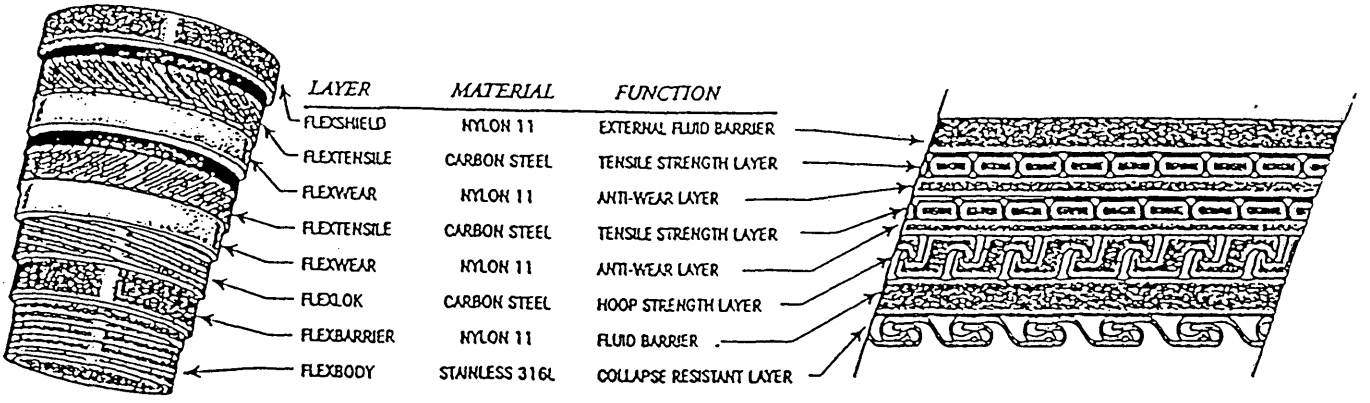

FIGURE 1
CROSS SECTION OF TYPICAL FLEXIBLE PIPE CONSTRUCTION AND LAYER DESCRIPTION

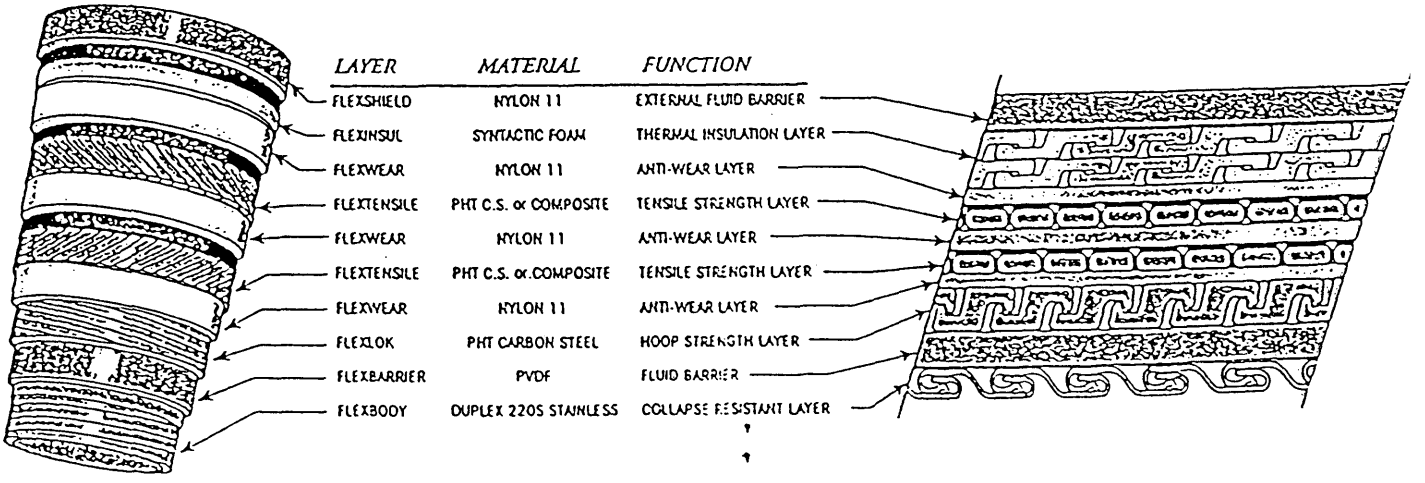

FIGURE 2
CROSS SECTION OF FLEXIBLE PIPE DESIGN USING ADVANCED MATERIALS

References for Chapter 1

1. McCullough, L. "Characterization of Nylon-11 Degradation," Master's Thesis, College of William & Mary, 1995.

2. Kalman, M. D., J. Belcher, and J. Plaia. "Advanced Materials for Flexible Pipe Construction." PD-Vol 53, *Offshore and Arctic Operations*, 1995. p 1.

3. Newbie, W. R. "*In Situ* Monitoring of Polymeric Degradation: Nylon-11 and PVDF," Honors Thesis, College of William and Mary, 1996.

4. Hood, D. K. "Monitoring and Modeling of Infiltration, Polymerization, and Degradation Phenomena in Polymeric Systems," Ph.D Dissertation, College of William and Mary, 1996.

5. Kalman, p 3.

Chapter 2. Chemistry of Nylon-11, PVDF, and Chemflake

Two materials, Nylon-11 and Poly(vinylidene fluoride), are examined in this study to determine the long-term aging condition and the feasibility for a more expanded use in off-shore oil platforms (see **Fig. 2.1**[1]). In order to understand and predict their response to testing conditions, a keen knowledge of the basic chemistry and properties of these polymers is essential.

I. Nylon-11, Rilsan

In the late 1920s, Wallace H. Carothers of Du Pont carried out the step polymerization studies that eventually led to the discovery of nylon-66, now a common polyamide used in textiles and coatings. His work not only expanded the use of synthetic organic chemistry to develop novel products, but he also revolutionized the advancement of polymer science which was held in skepticism during that time. Though nylon-66 and nylon-6

together account for approximately 90% of total nylon (or polyamide) output in the world, specialized types of nylon such as nylon-4,6, nylon-6,10, nylon-9, nylon-11, and nylon-12 are used for more rigorous environments.[2] Polyamides as a class in general offer high tensile strength, high impact strength, excellent fatigue resistance, and a good protection from a broad range of chemicals.

In this study, poly(imino-1-oxoundecamethylene) or nylon-11 (trade name Rilsan), is used:

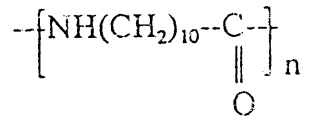

The main supplier of nylon-11 for this study is Elf-Atochem.

POLYMERIZATION OF NYLON-11

Nylon-11 is readily produced in quantity via self-condensation polymerization of ω-aminoundecanoic acid (obtained from castor oil) at around 220°C under pressure. Water is removed continuously in this condensation polymerization, which forces the reaction to rapid completion. Little, if any, isomerism is present since

the polymer is generally linear.

Nylons are typically semi-crystalline polymers. Along with amorphous regions, zones of crystallites are present due to the strong polarity that exists on the amide linkages. In addition, the linear regularity allows closely-packed lamellar crystalline structures to form in a fashion shown below:[3]

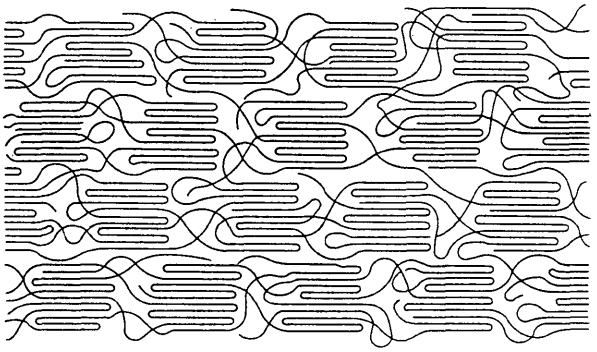

Figure 2.2 Crystallites within bundled lamellae

Such a structure is partly the reason why nylon is an appropriate material used for piping carrying crude oil. It would be quite difficult for hydrocarbons to traverse around the tortuous path of the nylon structure and therefore the vapor transmission rate with nylon is exceptionally low.[4]

Chemically, nylons offer strong resistance to

hydrocarbons, glycols, and bases, though they are susceptible to attacks by acids. Moreover, due to the high polarity of the amide linkages, nylons tend to absorb water much more so than other plastics. From **Table 2.1**, it is evident that nylon-11 is more useful under water since it absorbs much less water than the more widely used nylon-6 and nylon-66. This is because nylon-11 has a lower ratio of water-susceptible polar amide groups than the other two nylons.

DEGRADATION OF NYLON-11

As described above, nylons are vulnerable to attacks by acid and infiltration by water molecules. This acid-catalyzed hydrolysis of the amide bond is essentially the reverse of the condensation process (see **Fig. 2.3**). With the addition of the water across the amide bond and the resultant chain scission, molecular weight is noticeably reduced. This route of degradation is readily detected using methods of molecular weight determination, such as light scattering and solution viscometry.

The amorphous regions of the polymer are more susceptible to hydrolysis, which, when coupled with the shortened polymer chains through scission, increases the

overall crystallinity of the plastic. The higher crystallinity results in a drop of tensile strength along with flexibility. As the crystallinity increases, a lowering in the rate of hydrolysis is also expected. Therefore, it can be inferred that the initial stages of this aging study would yield the greatest changes in the physical properties of nylon through hydrolysis degradation.

II. Poly(vinylidene fluoride), PVDF

Polymers with fluorine substitutes are typically more stable to harsh environments than their unsubstituted counterpart hydrocarbon polymers. This can be attributed to the greater electronegativity of the fluorine atom, which in turn contributes to the high bond dissociation energy of the carbon-fluorine bonds on the polymer chain. Due to this unusually high thermal resistance of fluoropolymers, there was a great interest in the use of these materials beginning in the 1950s and 1960s for high temperature applications such as missile technology and space research.[5]

Given the repeating unit of polyethylene, $-CH_2-CH_2-$,

it is clear that fluorine can be substituted in up to four sites by replacing the hydrogens, giving rise to poly(vinyl fluoride), poly(vinylidene fluoride), poly(trifluoroethylene), and poly(tetrafluoroethylene). All four poly-fluorocarbon fibers have been manufactured to some extent, with the latter fluoropolymer poly(tetrafluoroethylene) or PTFE (Teflon) being the most widely used with numerous applications. Both PTFE and poly(trifluoroethylene) are difficult to fabricate into extruded parts; however, by giving up some corrosion and heat resistivity one can use the more tractable poly(vinylidene fluoride) and poly(vinyl fluoride).

There has been a greater interest in recent years in poly(vinylidene fluoride), or PVDF. This came about as a result of the discovery of the high piezo- and pyroelectric property present in certain forms of PVDF. Hundreds of references have been cited within the past five years with regard to this property of PVDF, since a high piezoelectric effect in a material allows it to be a potentially useful transducer by generating current with pressure or heat. PVDF has twice the amount of piezoelectricity as nylon-11, and properly prepared stretched PVDF films have been used as acoustic devices in

high-frequency speakers and headphones.[6]

In this continuous aging study, PVDF is used because it has relatively high mechanical strength and resistance to load deformation. In addition, it is even more chemically inert than nylon-11, again, due to the highly electronegative fluorine. Also, PVDF is much less water-absorbant compared to polyamides, which lessens swelling. With the right combination of plasticizers, the flexibility of PVDF can be improved for use in high temperature off-shore oil pipes.

POLYMERIZATION OF PVDF

Poly(vinylidene fluoride) is the addition polymer of vinylidene fluoride (VDF) or 1,1-difluoroethene. This monomer unit is a colorless and nearly odorless gas at room temperature and is readily prepared by the following methods:[7]

$$CH_3—CClF_2 \longrightarrow CH_2=CF_2 + HCl$$
$$CH_3—CBrF_2 \longrightarrow CH_2=CF_2 + HBr$$
$$CH_3—CF_3 \longrightarrow CH_2=CF_2 + HF$$
$$CH_2Cl—CClF_2 \longrightarrow CH_2=CF_2 + Cl_2$$

The first monomer precursor, 1-chloro-1,1-difluoroethane, is the preferred source and can be generated from

acetylene, vinylidene chloride, and 1,1,1-trichloroethane:

$$CH{\equiv}CH \xrightarrow{+2\,HF} CH_3{-}CHF_2 \xrightarrow{-Cl_2} CH_3{-}CClF_2 + HCl$$

$$CH_2{=}CCl_2 \xrightarrow{+2\,HF} CH_3{-}CClF_2 + HCl$$

$$CH_3{-}CCl_3 \xrightarrow{+2\,HF} CH_3{-}CClF_2 + 2\,HCl$$

VDF is primarily produced by Pennwalt Corp. in the United States, along with other producers in Japan (Daikin Kogyo) and Europe (Solvay & Cie, S.A. in Belgium).

The polymerization process of PVDF uses free-radical initiators in either suspension or emulsion. One type of PVDF studied in this project, Solef PVDF 1015/0078 supplied by Solvay-Wellstream, is suspension polymerized, which results in a lower dispersion of molecular weights than in an emulsion polymerization.[8] Furthermore, this material is plasticized to lower its melt viscosity and enable processing to be facile.

The end product typically has a high molecular weight (between 10^5 to 10^6 g/mol), with a 59.4 wt % of fluorine and 3 wt % of hydrogen. The high molecular weight correlates to the high tensile strength and durability of PVDF. Moreover, the polymer has a fair degree of crystallinity (35% to 70%), which is explained by its

tendency for head-to-tail configuration (>90%) along with the existence of a high amount of polarity (from the hydrogen and fluorine off the polymer backbone).[9]

These morphological distinctions greatly affect the solvent interaction and the dielectric behavior of PVDF. In fact, PVDF has a dielectric constant of around 7 (at 25°C and 60 Hz), which is unusually high for plastic materials.[10] Furthermore, four distinct crystalline polymorphs have been characterized in PVDF unlike most other synthetic polymers. These are α, β, γ, and δ, with the first two being the most commonly found forms. The alpha form is typical in normal melt-fabrication processes and has the trans-gauche conformation, while the beta form predominates in melt processes involving mechanical deformation and is slightly more dense. Depending on the proportions of these crystalline forms, the physical property of a sample of PVDF can vary quite dramatically. For example, different batches of resin have a melting range between 155°C and 192°C.[11]

DEGRADATION OF PVDF

When PVDF is irradiated or heated beyond normal processing temperature, the primary degradation route is

through the elimination of hydrogen fluoride with the formation of a conjugated polyene system.[12] This is evident through the detection of HF gas evolution as well as the darkening of the polymer from yellow to dark brown. At lower temperatures, intramolecular and intermolecular cross-linking predominates, depending on the environment. Degradation is typically complete after a maximum loss of one-third of its original weight. This weight loss stabilization is attributed to the substantial double bonds and cross-links in the polymer chain.[15]

Due to the chemical inertness of PVDF to a variety of compounds, it is difficult to speculate on the effect of how low concentrations of cleaning and stabilizing agents used in offshore oil pipes would affect the polymer over a period of time. These chemicals include various solvents for dissolving waxes and scales, as well as dehydrators and oxygen scavengers. Mechanisms for the degradation of PVDF, if present at all, through such a variety of chemical treatments have not been determined at this moment. As more molecular weight loss data is collected, the effect of these chemical fluids can be more firmly established.

III. Chemflake

Chemflake is a commercial glass-flake reinforced vinyl ester coating manufactured by Jotun Protective Coatings. It has been tested by the Research Center in Porsgrunn, Norway for use in coating steel acid holding tanks. Tests on various thicknesses of coating of Chemflake revealed slow penetration of concentrated HCl after 18 months of study at 45-55°C.[16]

SAMPLE PREPARATION

The Chemflake coating used in this study was supplied by Jotun. All components of the mixture were kept in a freezer until ready to be used.

There are four components required to make a batch of Chemflake. The first part is the Chemflake Base, which is a off-white thick liquid composed primarily of styrene, polyester resin, and glass flakes fillers. To the base is added Norpol Accelerator 9802, a purple liquid containing styrene, xylene, and coboltoctate. Norpol Accelerator 9826, a solution of styrene and N.N.-Dimethylaniline, is added next. The mixture is stirred thoroughly at this

point. The last part of the recipe calls for Norpol Catalyst (also known as Baltoflake B), which contains predominantly Methyl Ethyl Ketone Peroxide.

After mixing in the final component, the Chemflake begins to harden. Within hours, it becomes hard and brittle and can be quite difficult to remove from the mixture container. Small amounts of Chemflake can be dissolved by xylene, but any thicker layers will require a lengthy soak in either xylene or acetone to remove effectively.

APPLICATIONS

As mentioned previously, Chemflake is used commercially as a protective tank lining, predominantly for holding HCl used in the PVC industry. Since PVC alone accounts for a majority of polymers used around the world, it is crucial that effective holding tanks be build to hold large amounts of HCl. The use of Chemflake allows relatively inexpensive and high strength steel to be used for such a purpose.

Figure 2.1 Rotary and Offshore Drilling Rigs[1]

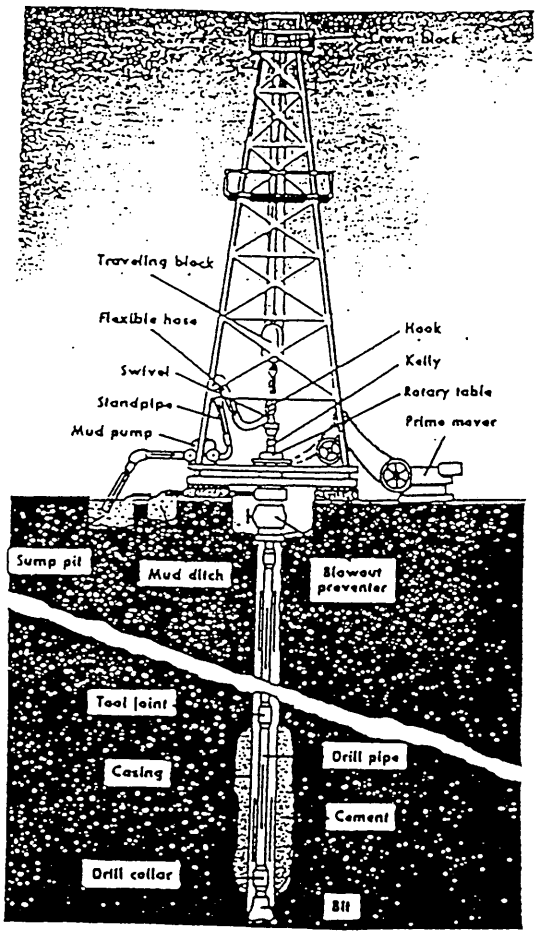

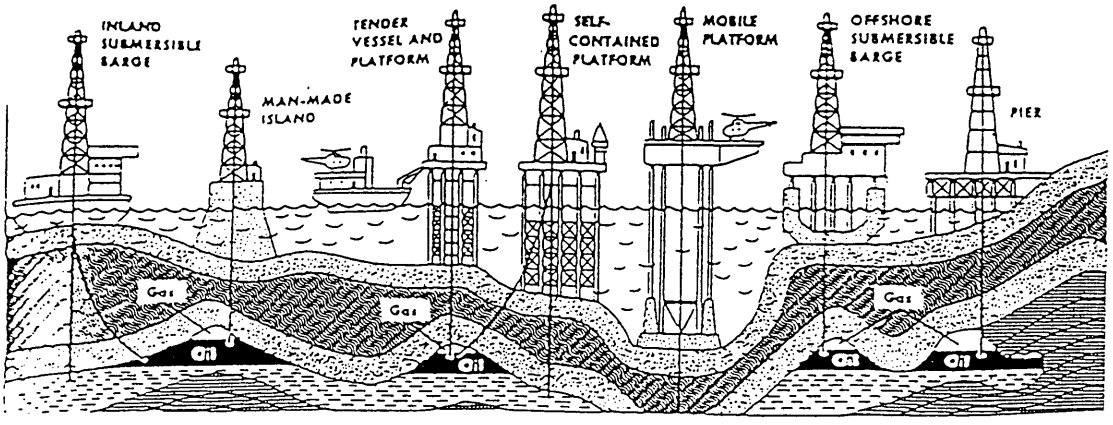

Table 2.1 Various Properties of Nylon Plastics[13]

Polymer Resin	Number of $-CH_2-$ Groups	Weight Fraction of $-CH_2-$ Groups in Chain	Melting Temperature		Deflection Temperature under 66 psi Load (455 kPA)		264 psi Load (1.82 (MPa)		Water Absorption (saturation at R.T.) (%)
			°F	°C	°F	°C	°F	°C	
Nylon 6	5	0.71	440	225	360	182	160	71	9.5
Nylon 11	10	0.83	375	190	302	150	131	55	1.9
Nylon 12	11	0.85	355	180	302	150	135	57	1.5
Nylon 6/6	6/4	0.71	510	265	470	243	220	104	8.5
Nylon 6/10	6/8	0.78	435	225	300	149	135	57	3.3
Nylon 6/12	6/10	0.80	410	210	—	—	—	—	2.8
Polyethylene (high density)	5000+	1	275	135	185	85	—	—	<0.01

Figure 2.3 Acid-Catalyzed Hydrolysis of an amide bond[14]

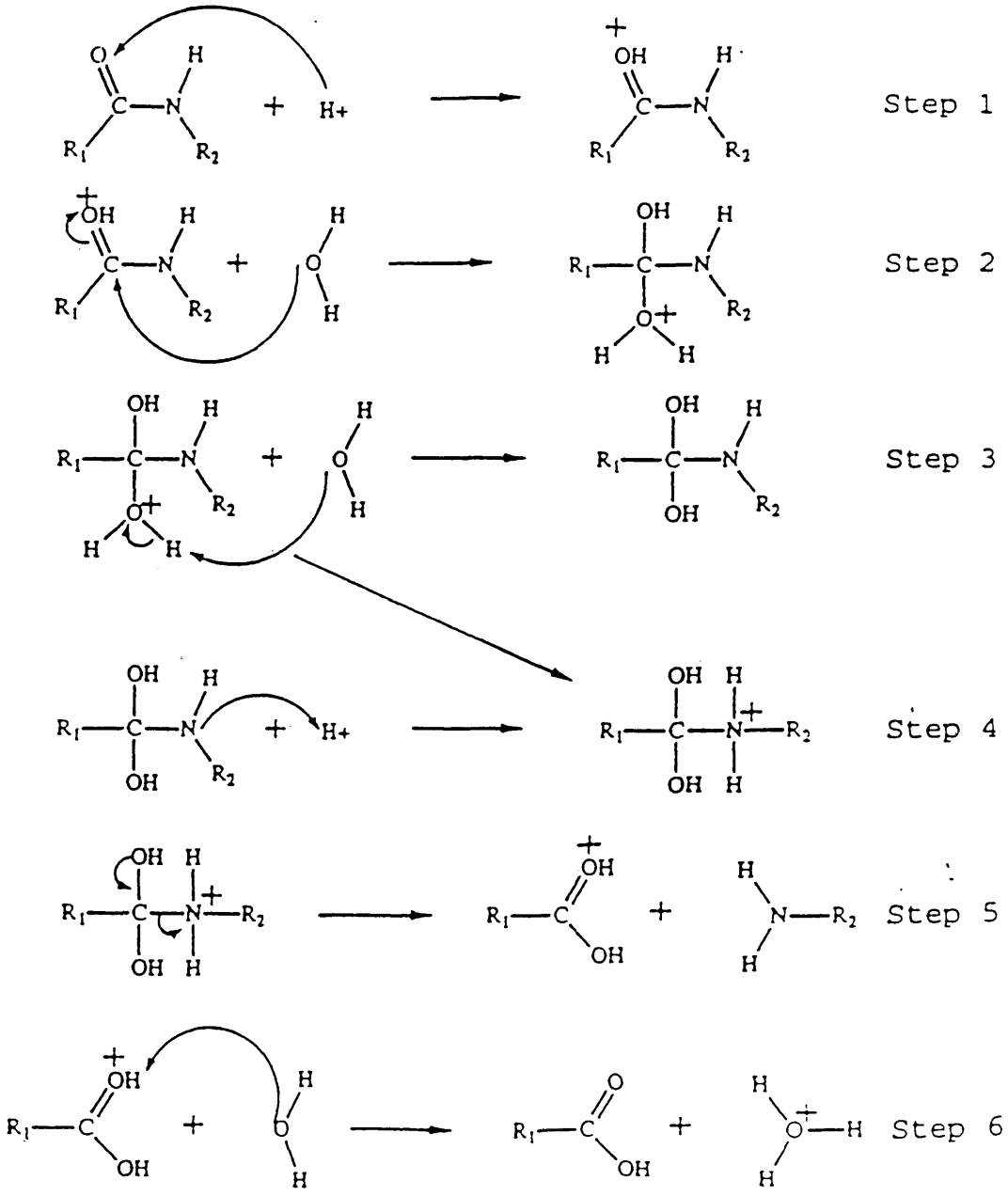

References for Chapter 2

1. Collier's Encyclopedia, 1987. Vol. 17; pp 647 & 649.

2. Hall, Christopher. Polymer Materials. 2nd edition. New York: John Wiley & Sons, 1989. p 216.

3. Van Krevelen, D. W. Properties of Polymers. 2nd edition. New York: Elsevier Scientific Publishing Company, 1976. p 29.

4. Gruenwald, G. Plastics. New York: Hanser Publishers, 1993. p 131.

5. Nguyen, T. Degradation of Poly(vinyl Fluoride) and Poly(vinylidene Fluoride). JMS-Rev. Macromol. Chem. Phys., 1985. C25(2); p 228.

6. Seymour, Raymond B. Polymers for Engineering Applications. ASM International, 1987. p 105-106.

7. Mark, Herman F. *et al.* Encyclopedia of Polymer Science and Engineering. 2nd edition. New York: John Wiley & Sons, 1989. Vol. 17; p 533.

8. Kalman, M. D., J. Belcher, and J. Plaia. "Advanced Materials for Flexible Pipe Construction." PD-Vol 53, *Offshore and Arctic Operations*, 1995. p 1.

9. Mark, p 532.

10. Gruenwald, p 254.

11. Mark, p 538.

12. Nguyen, p 231.

13. Gruenwald, p 108.

14. Hood, D. K. "Monitoring and Modeling of Infiltration, Polymerization, and Degradation Phenomena in Polymeric Systems," Ph.D Dissertation, College of William and Mary, 1996.

15. Nguyen, p 268.

16. Jahnsen, Thor H. Summary of Long-Term Testing of Chemflake; Porsgrunn, Norway, 1993.

CHAPTER 3. Experimental Techniques

Various experimental techniques were employed in the study of the aging of nylon-11, PVDF, and Chemflake. Frequency dependent electromagnetic sensing and viscosity measurements were taken with a primary focus, though of equal importance were the use of DSC, mechanical testing, hardness testing, and weight loss measurements. It is imperative to understand the importance of using all of the above techniques in order to correlate the data with the lifetime monitoring of the particular polymer in its service condition.

I. FREQUENCY DEPENDENT ELECTROMAGNETIC SENSING (FDEMS)

Frequency dependent electromagnetic sensing, or FDEMS, is an useful technique of relating the microscopic behavior of the material in question with its macroscopic properties. It has the quality of continuous *in situ* monitoring of the cure and degradation processes of the

polymeric system. In addition, it is convenient and has good reproducibility, sensitivity, and the capability for remote sensing.[1] FDEMS utilizes impedance measurements involving a range of frequency from tens of hertz to the megahertz region to monitor molecular motion. The FDEMS sensor patented by Kranbuehl, shown below, consists of two finely interdigitated comb electrodes composed of noble metals and high temperature ceramics laid on either glass or Kapton, which are both geometry independent. The interdigitated combs basically represent parallel plate capacitors in this case.

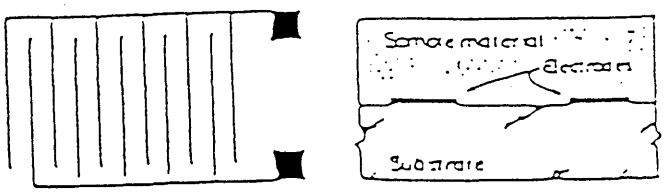

Figure 3.1 Impedance measurement sensor.

Capacitance

A useful capacitor consists of closely-spaced parallel conducting plates. The charges present on the

plates with an applied voltage V, assuming equal geometry and material, can be called $+Q$ and $-Q$, as seen in Figure 3.1.[2]

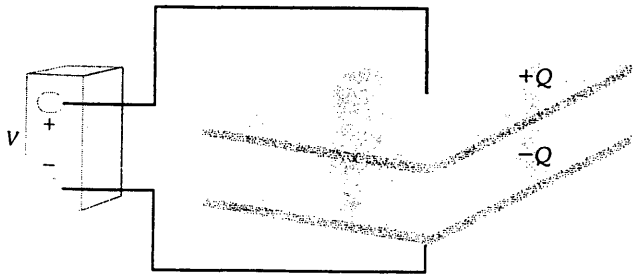

Figure 3.2 A capacitor.

The capacity for a particular material to store charge for a given potential difference is termed capacitance and given as

$$C = \frac{Q}{V} \qquad [3.1]$$

Note that if the distance d between the plates is small compared to the area of the plates, the electric field experienced by a point on one plate from the other plate can be viewed as a field near an infinite plane of charge with a surface charge density σ, which is simply the

charge per unit area:

$$\sigma = \frac{Q}{A} \qquad [3.2]$$

According to Gauss's law, the net flux (E_n) through any surface (S) is equal to $4\pi k$ times the total charge within the surface:[3]

$$\phi = \oint SE_n \, dA = 4\pi k Q_{inside} \qquad [3.3]$$

It is more common to write the Coulomb constant k in terms of the permittivity of free space ϵ_o:

$$k = \frac{1}{4\pi\epsilon_o} \qquad [3.4]$$

So **equation 3.3** can be rewritten as

$$\phi = \oint SE_n \, dA = \frac{1}{\epsilon_o} Q_{inside} \qquad [3.5]$$

Rearranging **equations 3.2** and **3.5** (accounting for flux through both sides of the surface), the following is derived:

$$2E_n A = \frac{1}{\epsilon_o} \sigma A \qquad [3.6]$$

Solving for E_n in **equation 3.6** and multiplying by two for the number of plates, the following is obtained:

$$E = \frac{\sigma}{\epsilon_o} \qquad [3.7]$$

The potential difference in this parallel-plate capacitor would equal the applied electric-field multiplied by the distance between the plates. Substituting in **equations 3.7** and **3.2**, the result is

$$V = Ed = \frac{\sigma}{\epsilon_o} d = \frac{Qd}{\epsilon_o A} \qquad [3.8]$$

Going back to **equation 3.1**, the capacitance of the parallel plate is derived:

$$C = \frac{Q}{V} = \frac{\epsilon_o A}{d} \qquad [3.9]$$

where ϵ_o equals 8.85 x 10^{-10} Farads per centimeter.

POLARIZATION

When a dielectric material is placed between the capacitor plates, the charge increases for the same voltage due to polarization of the dielectric. Figure 3.3 shows several mechanisms of polarization due to an applied electric-field.[4]

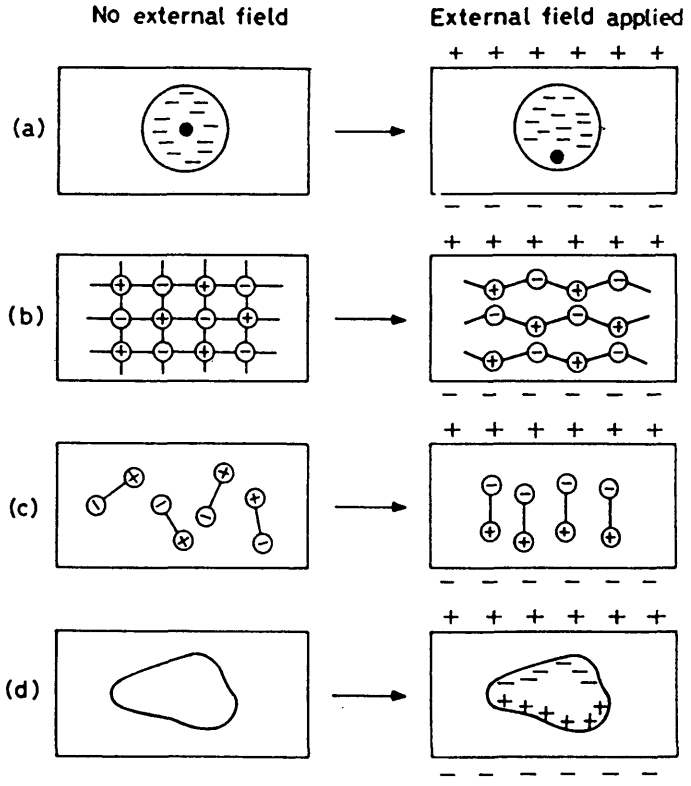

Figure 3.3 Polarization mechanisms.

From **Fig. 3.3a**, the atom can be viewed as a cloud of negative charge surrounding a positive nucleus. With no

external field, the resultant net dipole is zero for the atom. Once a field is applied, the nucleus and the negatively charged cloud each become attracted to their respective oppositely-charged plates, resulting in what is called an electronic polarization.

It is evident that as the volume of the electron cloud grow larger, the atom becomes easier to be electronically polarized. This is shown in the equation for ***dipole moment*** μ

$$\mu = (4\pi\epsilon_o R^3)E = \alpha_e E \qquad [3.10]$$

where α_e is called the electronic polarizability and is a constant for that specific atom. The polarizability is proportional to the volume of the electron cloud in **equation 3.10.**

For a polar molecule, a permanent dipole exists since the centers of the negatively charged electron cloud does not coincide with the center of the nucleus. In any case, with an applied electric-field E in the parallel-plate capacitors mentioned above, polarization takes place within a sample placed between the plates. Since dipole moment is directly related to the polarization (which is

equivalent to the dipole moment per unit volume), examining the various mechanisms which give rise to the different types of polarization, seen in **Eq. 3.11**, is crucial to understanding the frequency dependence of the dielectric constant.

$$P = P_e + P_i + P_o + P_s \qquad [3.11]$$

P_e is the ***electronic polarization*** due to the shifting of the electron cloud in response of an atom or ion to an electric-field. P_i, the ***atomic polarization***, is the displacement of atoms due to the applied field. P_o is called the ***orientation polarization*** and is seen commonly with materials having polar molecules, since they are more likely to be oriented in an electric-field. The ***interfacial polarization*** (also called ***space charge polarization***), P_s, is due to the shifting of whole phases of ionic charges within the body of the dielectric material.[5]

Dielectric Constant

As a dielectric material is inserted between the capacitor plates with field E, the dipoles (induced and

permanent) align as seen in **Fig. 3.4.**[3]

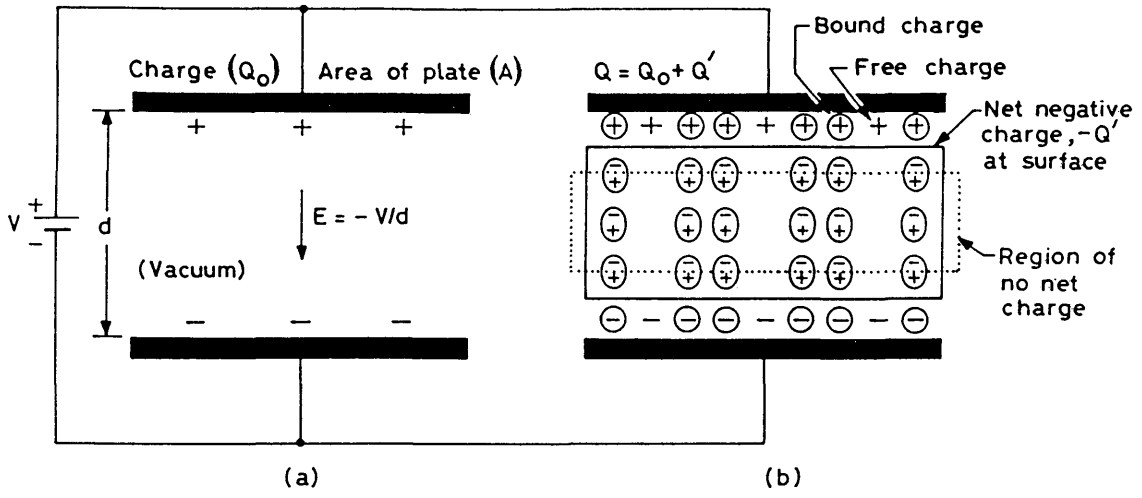

Figure 3.4 Effect of dielectric material within a capacitor

As mentioned previously, the polarization of the dielectric material increases the total charge, which in turn gives rise to a term called the ***relative permittivity*** or ***relative dielectric constant***, ϵ_r:

$$\epsilon_r = \frac{Q}{Q_o} = \frac{\epsilon}{\epsilon_o} = \frac{C}{C_o} \qquad [3.12]$$

This value is always greater than one since it compares an increased capacitance (due to the dielectric) with the capacitance in vacuum.

Now consider a dipole within the material. As the electric field is applied, the various polarization mechanisms take place. Suppose the direction of the field is reversed 180°, the dipole will attempt to re-align itself with the new field. This, however, takes a finite amount of time. So as the frequency of the field reversal increases, there will be a certain frequency above which the dipole simply cannot keep up with the alteration of direction. Above this frequency, often referred to as the ***relaxation frequency***, the loss of polarization from the dipole diminishes the effective dielectric constant of the material.

The relaxation frequency of interfacial polarization is relatively low (around 10^3 Hz) since a large body of ionic charge must move through the matrix of the dielectric material, which is fairly resistive. Dipole orientation of polar groups has relaxation frequencies slightly higher, slightly above the radio-frequency region. Atoms have much less inertia and tend to vibrate with thermal energy, which correspond to relaxation frequencies around the infrared region for the atomic polarizations. Electrons, with even smaller mass and inertia, can easily vibrate with the fluctuating field and

thus do not relax until around 10^6 Hz (near the ultraviolet region). Though electronic polarization is present in a wide range of frequency, its effect does not contribute as much to the permittivity compared to the other types of polarization mechanisms below the megahertz region.

Using the Kranbuehl impedance measurement sensor, the permittivity of the material can be measured and calculated. The complex relative permittivity, ϵ^*, is described as

$$\epsilon^* = \epsilon' - i\epsilon'' \qquad [3.13]$$

where ϵ' and ϵ'' represent the dielectric permittivity (real component) and the loss factor (imaginary component) and are calculated from

$$\epsilon' = \frac{C}{C_o} \qquad \epsilon'' = \frac{G}{C_o\omega} \qquad [3.14]$$

Both the capacitance, C, and the conductance, G, values are measured and read with an impedance bridge. As mentioned previously, four mechanisms of polarization contribute to the overall response of a material to an

electric-field. Using frequencies between 1 kHz and 1 MHz, both the ionic (from interfacial polarization) and dipolar components of polarization are examined, while the atomic and electronic polarizations do not relax at such low frequencies and merely contribute to the background of the complex permittivity. The ionic portion tends to dominate at low frequencies, as well as low viscosities and high temperatures. Conversely, the dipolar component is seen at high frequencies and higher viscosities.

From the time dependence of the real permittivity and the loss factor, both the ***ionic mobility*** σ and the ***dipolar mobility*** τ of the material can be examined. Both parts of ϵ^* can be described in terms of their ionic and dipolar portions:

$$\epsilon' = \epsilon'_d + \epsilon'_i \qquad [3.15]$$

$$\epsilon'' = \epsilon''_d + \epsilon''_i \qquad [3.16]$$

τ can be experimentally determined using the Cole-Davidson function:[5]

$$\epsilon_d^* = \epsilon_\infty + \frac{\epsilon_o - \epsilon_\infty}{(1 + i\omega\tau)^\beta} \qquad [3.17]$$

where ϵ_o and ϵ_∞ are limiting low and high frequency values of the complex permittivity, and β is the relaxation time distribution parameter. An empirical equation was derived by Johnson and Cole in determining σ:

$$\epsilon_i'' = \frac{\sigma}{\epsilon_o \omega} - C_o Z_o \cos\frac{(n\pi)}{2} \omega^{-(n-1)} \left(\frac{\sigma}{\epsilon_o}\right)^2 \qquad [3.18]$$

The second term of **Eq 3.18** is due to electrode charge polarization, which is a complicated effect that is only a contributing factor below 10 Hz and therefore can be discarded for the frequencies measured (kilohertz to megahertz region). **Eq 3.18** can therefore be reduced to

$$\epsilon_i'' \cong \frac{\sigma}{\epsilon_o \omega} \qquad [3.19]$$

The understanding of both σ and τ provide insightful knowledge into the advancement of polymerization and the cure process of the material under study.

II. Solution Viscometry

The viscosity of a fluid can be defined as the resistance to flow between parallel layers within a stationary fluid when a shearing force is applied:[6]

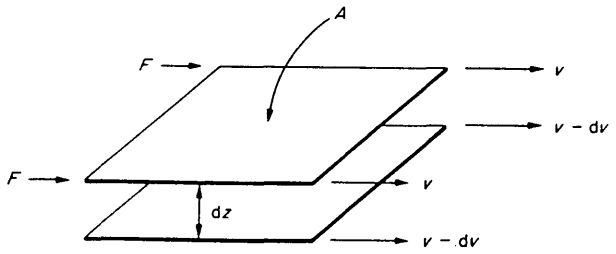

Figure 3.5 Fluid Flow Representation

In a Newtonian fluid, the viscosity η is the proportionality constant that relates laminar flow and shear stress.

When a polymer is dissolved in a solvent, the solution becomes more viscous due to the large difference in size between the polymers (high molecular weight) and the solvent molecules (low molecular weight).. By comparing the ratio of the dynamic viscosity between the pure solvent and the dilute polymer solution, the relative size of the polymer can be determined. In turn, the molecular weight can be estimated. Though this method is

not absolute, solution viscometry is a quick and inexpensive way for characterizing the polymer in solution.

VISCOMETERS

The measurement of a viscosity solution sample is made using a capillary viscometer, several of which are shown below:[7]

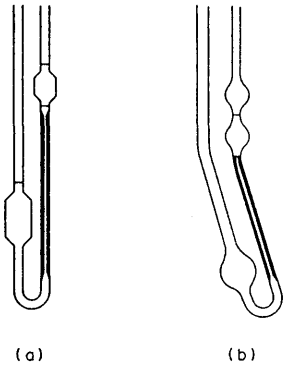

U-tube viscometers: (a) Ostwald, (b) Cannon–Fenske

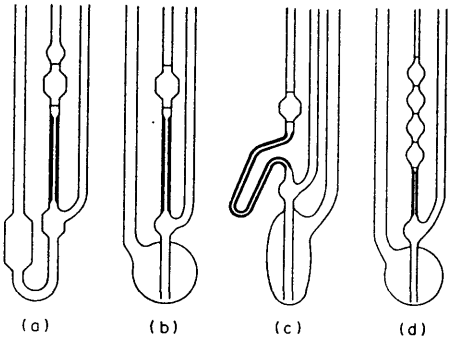

Suspended levei viscometers: (a) Ubbelohde; (b) modified Ubbelohde; (c) Desreux–Bischoff type; and (d) Schurz–Immergut type

Figure 3.6 Viscometers.

Of these, the Ostwald and the Ubbelohde types are the most commonly used. The suspended level viscometers have an advantage over the U-tube viscometers in that the driving force for the flow of fluid through the capillary tube is not affected by the amount of liquid originally introduced. For this reason, Ubbelohde viscometers are utilized in this study.

TREATMENT OF DATA

The time required for a viscosity sample to run through two marks on the viscometer is measured using a Fisher lab timer. The temperature must remain as constant as possible, since a change of a degree from 20°C represents a viscosity change of 1 to 2%.[7] The constant temperature bath used in this study was set at 25°C with an observed fluctuation of less than 0.1°C for different measurements.

The relationship between the measured flow time for a sample with the pure solvent time is called the ***relative viscosity*** (IUPAC ***viscosity ratio***), η_r:[8]

$$\eta_r = \frac{\eta}{\eta_o} = \frac{t}{t_o} \qquad [3.20]$$

This is a simplified way to examine viscosity neglecting kinetic energy corrections, seen in **Eqns 3.21** and **3.22** (where A and B are constants):[9]

$$\Delta = \sum_{n=1}^{\infty} \left(\frac{B}{At_o^2}\right)^n \qquad [3.21]$$

$$[\eta] = [\eta]_{expt}(1 + 2\Delta) \qquad [3.22]$$

This correction term is derived empirically to compensate for the change in kinetic energy resulting from convergence and divergence of liquid flow lines passing through a capillary tube. The term **2Δ** can be neglected by restricting the width of the capillary tube as much as possible to ensure a small volumetric flow rate, which increases $\mathbf{t_o}$ in **Eqn 3.21** and diminishes **Δ**.

It is appropriate now to introduce the ***specific viscosity*** term η_{sp}:

$$\eta_{sp} = \frac{\eta - \eta_o}{\eta_o} = \eta_r - 1 \qquad [3.23]$$

Both η_r and η_{sp} are concentration-dependent; as the concentration of the polymer in the solution increases, both of the viscosity terms increase. This dependence is better described by ***reduced viscosity*** (IUPAC ***viscosity number***), η_{red}:

$$\eta_{red} = \frac{\eta_{sp}}{C} \qquad [3.24]$$

From **Eqn 3.24**, another term can be generated:

$$[\eta] = \lim_{c \to 0} \left(\frac{\eta_{sp}}{C}\right) = \lim_{c \to 0} (\eta_{red}) \qquad [3.25]$$

where $[\eta]$ is called the ***intrinsic viscosity*** (IUPAC ***limiting viscosity number***) and is the limit of the reduced viscosity as the concentration approaches zero.

For a given solvent and temperature, it is possible to correlate the intrinsic viscosity to the molecular weight of the polymer through the Mark-Houwink equation:[10]

$$[\eta] = KM_V^a \qquad [3.26]$$

Both K and a are constants (for a particular solvent and temperature) obtained from calibration plots, and can be

readily obtained from various literature sources. The solvents used in this study are *m*-cresol for nylon-11 and 2,2-Dimethylacetamide (DMAC) for PVDF.

The molecular weight obtained from **Equation 3.26** indicates only the average viscosity weight and is validated by running the sample until a close agreement in the measured time is acquired.

III. Differential Scanning Calorimetry (DSC)

Differential scanning calorimetry is a useful method for determining several physical constants of polymers through heating and examining the enthalpies of transition processes. These include T_g, melting point, and degree of crystallinity.

The apparatus, called the differential scanning calorimeter, is designed to determine the enthalpies of these various processes by measuring the differential heat flow required to maintain a material sample and an unreactive reference at the same temperature.[11] As a sample goes through a transition, heat is either absorbed or given off. The change in the current flow at this transition can be easily monitored to a precise degree.

This is accomplished by using individual electric heaters monitored by sensitive sensors (which regulates current flow into the reference and sample pans) to adjust the input of heat, as seen below:[12]

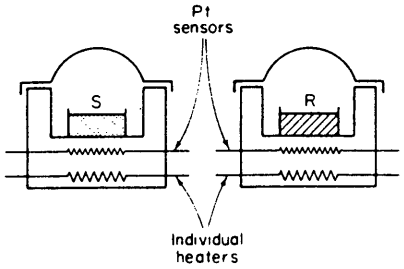

Figure 3.7 DSC System.

A characteristic DSC scan may show a curve similar to **Fig. 3.8**, where T_g is the glass transition temperature (a second-order transition) and T_m is the melting temperature (a first-order transition):[13]

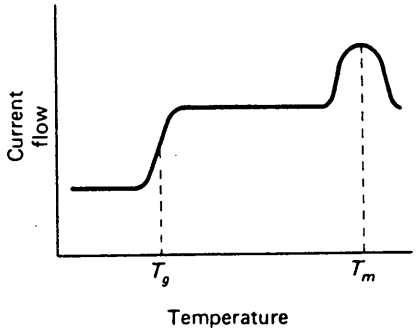

Figure 3.8 An Ideal DSC Scan.

Scans in this study were taken on a Perkin-Elmer DSC-

7 instrument. Each sample requires between 5 and 10 milligrams crimped inside an aluminum pan; the small size of the sample confined within the pan helps reduce thermal resistance so heating lag is minimized.

Once a scan is complete, the enthalpy ΔH_{melt} can be calculated through the integration of the total peak area. This value can be compared to the enthalpy of a sample that is entirely crystalline, which is the ΔH^{o}_{melt}. The relationship between the two is termed the ***percent crystallinity***:

$$\% \, Crystallinity = \frac{\Delta H_{melt}}{\Delta H^{o}_{melt}} \, x \, 100 \qquad [3.27]$$

The ΔH^{o}_{melt} of Nylon-11 is 54.1 cal/g (226 J/g), while the ΔH^{o}_{melt} of PVDF is 92.9 J/mol.[14,15]

Similarly, the advancement of the polymerization process of a material can be examined after a dsc run. Using an integration program, the area of the exotherm can be determined. This area represents the heat of reaction given off as the polymer is heated. The degree of cure, α, at anytime is simply the heat of reaction at that time divided by the total heat of reaction.

IV. Hardness Testing

Hardness measurement is a simple, nondestructive method of examining another physical property of a material. The most common method for testing the hardness of a plastic is by examining its resistance to indentation. Types of hardness tests using this method include Brinell, Vickers, Knoop, Rockwell, Barcol, and Durometer hardness.

In this study, the Barcol hardness is measured using a Barber Coleman impressor (Model GYZJ-935). This instrument, shown in **Fig. 3.9**[16], is a hand-held unit that is simple to operate.

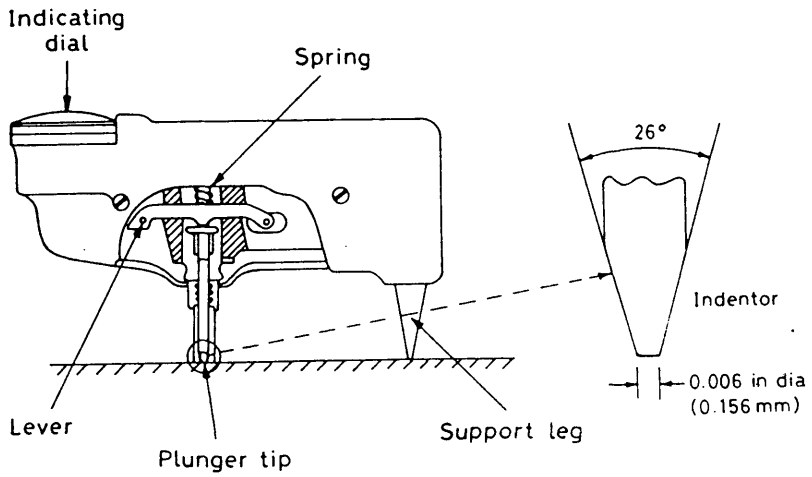

Figure 3.9 Barcol Hardness Tester.

By supporting the back leg of the device and firmly pressing the spring-loaded indentor onto the substrate, a hardness number can be read off the dial.

Typically, a measurement is taken only after allowing the tester to be held in place for 10 seconds. This is necessary due to the amount of creep present in most plastics. The hardness number has no unit. Rather, it can be compared to other test numbers and even tests done on other types of hardness testers.

V. Mechanical Testing of Tensile Strength

Mechanical tensile tests were performed on a United SFM-10 tensile test apparatus at NASA Langley for the purposes of this study. These measurements were done according to the American Society for Testing and Materials (ASTM) test method D638-87b. The dimensions of the mechanical sample are: thickness = 0.229 in., total length = 5.25 in., width = 0.47 in., gage length = 2.5 in, and gage width = 0.243 in.

The sample is gripped in place as shown on the following page:[17]

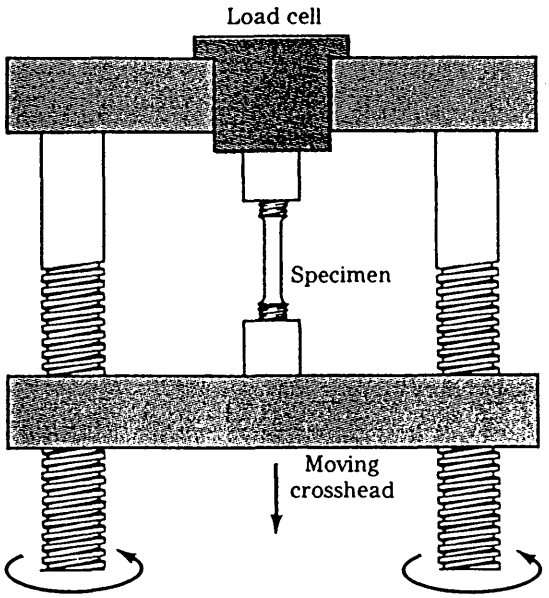

Figure 3.10 Operation of Tensile Machine.

As the sample is pulled (at a constant speed of 0.5 in/min for the nylon-11 sample), the gage length (L) increases as the gage width (a) decreases as seen in **Fig. 3.11.** The tensile strength of the specimen seen in the figure is equal to the load divided by the cross sectional area of the gage area being tested, or

$$\epsilon = \frac{F}{a \times b} \qquad [3.28]$$

while the percent elongation is calculated as

$$\%\ Elongation = \frac{(L_2 - L_1)}{L_1} \times 100\% \qquad [3.29]$$

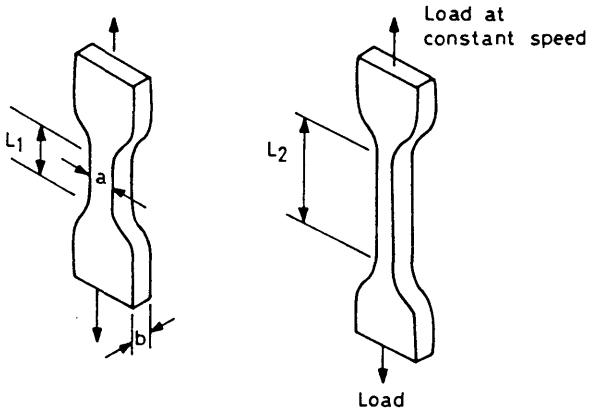

Figure 3.11 Schematic of Tensile Test Sample.[18]

Plotting the stress (tensile strength) versus the strain (elongation), a plot such as the one shown in **Fig. 3.12** is derived. The part of the curve that lies on the straight line drawn to the origin represents the region of elastic strain. This means that the polymer can stretch and return to its original dimensions as long as the

stress applied does not go above the point where deviation from linearity occurs. Beyond that point, plastic deformation (irreversible change in dimensions) occurs. Since the point where the elastic region ends and plastic deformation begins is not clear most of the time, it is standard in American engineering tests to set the ***yield strength*** as the tensile strength at 0.2 percent offset (elongation). From **Fig 3.12**, a 0.2 percent offset yield strength of approximately 78,000 psi is derived by drawing a line parallel to the linear portion of the curve from 0.002 in./in. strain to the intersection with the upper portion of the curve.

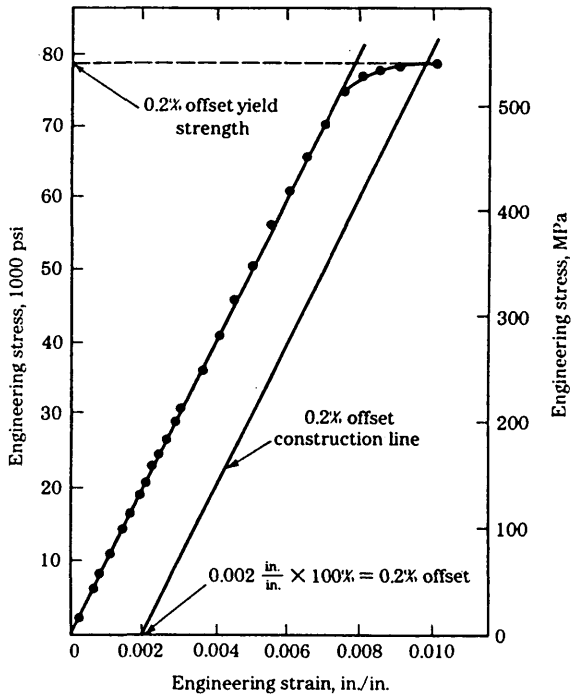

Figure 3.12 Stress-Strain Diagram.[19]

From this diagram, it is also possible to determine the load at break and percent extension at break. For nylon-11, most of these data have been tabulated. A new MTS Mechanical Testing System has recently been acquired and is located at the College of William and Mary. It will not be available for mechanical testing of PVDF at the time of the writing of this thesis.

VI. Weight Change

Another important issue that needs to be dealt with in this project is the plasticizer content of the materials being tested. Plasticizer is needed to soften the material for easy processing. Materials become more flexible with added plasticizer because these small molecules tend to break up crystallinity that is present. This allows the polymer chains to undergo reptation with more ease and therefore the polymer becomes more tractable.[20]

Both nylon-11 and PVDF have a significant amount of plasticizers within them. For example, the Solef PVDF 1015, the plasticized form that is used in this project has a percent elongation at break of up to 385% at room

temperature, while the unplasticized compound only has a percent elongation at break of 46%.[21]

References for Chapter 3

1. Kranbuehl, D., D. Hood, L. McCullough, H. Aandahl, N. Haralampus, and W. Newby. "Frequency Dependent Electromagnetic Sensing (FDEMS) for Life Monitoring of Polymers in Structural Composites During Use." 1995, in press.

2. Tipler, Paul A. Physics. New York: Worth Publishers. 1991. p 691.

3. Tipler, p 625-630.

4. Chanda, Manas and R. K. Salil. Plastics Technology Handbook, 2nd edition. New York: Marcel Dekker, Inc. 1993. p 317.

5. von Hippel, Arthur. Dielectric Materials and Applications. Cambridge: The M.I.T. Press. 1954. p 19.

6. Lovell, Peter A. "Dilute Solution Viscometry". *Comprehensive Polymer Science, Volume 1*. New York: Pergamon Press. 1989. p 174.

7. Lovell, p 175.

8. Allcock, Harry R. and F. W. Lampe. Contemporary Polymer Chemistry. Englewood Cliffs: Prentice-Hall, Inc. 1990. p 383.

9. Lovell, p 177.

10. Sperling, L. H. Introduction to Physical Polymer Science. New York: John Wiley & Sons, Inc. 1992. p 104.

11. McNaughton, J. L. and C. T. Mortimer. Differential Scanning Calorimetry. Reprint from "IRS; Physical Chemistry Series 2, 1975, Volume 10". London: Butterworths. p 2.

12. McNaughton, p 3.

13. Allcock, p 433.

14. Inoue, M. "Studies on Crystallization of High Polymers by Differential Thermal Analysis." Journal of Polymer Science, Part A. New York: John Wiley &

Sons, Inc., 1963. p 2700.

15. Welch, Gordon, and Robert Miller. Journal of Polymer Science, Polymer Physics Edition. **Vol. 14**, p 1683.

16. Chanda, p 287.

17. Smith, William F. Foundations of Materials Science and Engineering, 2nd edition. New York: McGraw-Hill, Inc., 1993. p 201.

18. Chanda, p 339.

19. Smith, p 205.

20. Sperling, p 314.

21. Kalman, M. D., J. Belcher, and J. Plaia. "Advanced Materials for Flexible Pipe Construction." PD-Vol 53, *Offshore and Arctic Operations*, 1995. p 5-6.

CHAPTER 4. Experimental Setup and Results

Setting up the FDEMS sensor requires embedding the glass (or Kapton) probe within the material being tested. It is important to allow the polymer to fully cover the entire sensor, and it is essential that the sensor is totally embedded within the polymer tested so that its outer environment can only reach the probe through diffusion into the material.

Nylon-11

Both PVDF and Nylon-11 are supplied to this lab in the form of extruded pipes. Using a heated hydraulic press, a sample cut off the pipe is heated to flow and gradually flattened to a 1/4 inch thick piece. Using a silver two-part epoxy, teflon-coated copper wires are attached onto the active sensing area of the FDEMS sensor and cured at 200°C. The sensor is carefully set between two pieces of the flattened pipe and reheated in the

hydraulic press. The final polymer sample with the sensor embedded in the middle is approximately 3/8 inch thick.

Prior to immersing the FDEMS sample into the environment to be tested, it is held in place by sandwiching the material (with the sensor in it) between two steel plates with holes drilled in them. The plates prevent the polymer from warping and cracking the sensor, while the holes allow the material to interact fully with its environment.

In addition to using the 1/4 inch panels for FDEMS samples, strips of smaller pieces are also cut for other testing purposes, such as periodic viscosity and DSC sampling as well as frequent hardness and weight loss measurements.

Prior to this phase of study involving nylon-11, several sensors were placed in three pots of various water-oil concentrations at 105°C. The results of these FDEMS sensor tests along with various physical and mechanical tensile tests were given in **Refs. 1-3.**

In this work, a new FDEMS sensor for nylon was made and placed in a bath of 95°C 95% IRM-903 oil (supplied by R. E. Carroll, Inc.) and 5% de-ionized water charged with CO_2. IRM stands for *Industry Reference Materials*, and

IRM-903 oil has been adopted by an ASTM committee within the past few years to replace previous testing oils due to its high homogeneity.[4] The aqueous portion of the mixture becomes acidic (pH=4.5) after bubbling carbon dioxide through the mixture for an hour.

FDEMS data gathered over a period of time in this particular environment was averaged and merged. FDEMS sensor plots of the **log ϵ'** and **log (ϵ'' x ω)** over the entire duration of the run are shown in **Fig. 4.1** and **4.2.** There was a glitch in the heating system after 40 days which caused a temperature increase of 10°C, which explains the slight elevation in the ϵ'' values (indicating greater ionic mobility) at around 50 days. Otherwise, the plot provides a good representation of a typical FDEMS output: the initial jump of all the frequencies as the sensor is placed in the oil-water bath indicates diffusion of water into the material, while the gradual decline of **log (ϵ'' x ω)** as the nylon ages signifies a loss of ionic mobility as a result of increasing rigidity (due to an increase in the degree of crystallinity as the molecular weight decreases).

An important aspect of this phase of study was the effect of acidity and water-cut at different temperatures

on the molecular weight of nylon-11. In Chapter 2, the principal route of degradation in nylon-11 was attributed to acid-catalysis. Using de-ionized water (pH=7), SB104-1 buffer from Fisher Chemicals(pH=6.0), and CO_2-charged water (pH=4.5), nylon samples were placed in sealed pressure test tubes and allowed to age at 70°C, 90°C, 105°C, and 120°C. Since the initial studies began at 105°C, all of the previous data gathered were at this temperature. By Fall 1996 all of the data at the new temperatures should be compiled. A listing of the various types of environments tested in this study is shown on **Table 4.1.** The one environment at 130°C was part of the earlier Phase I study.

Molecular weight was measured periodically and the results are shown in **Table 4.2** for various conditions at 105°C. Additional molecular weights at other temperatures are shown in **Table 4.3.**

Plots of *MW vs Days and Log MW vs. Days*, seen in **Figs. 4.3** and **4.4**, show that varying conditions between pH = 7 and pH = 4.5 does not appear to have a significant effect on the rate and extent of degradation in nylon. This is quite unexpected considering that degradation of

nylon in aqueous media is acid catalyzed.

Figs. 4.5 and **4.6** show the rate of molecular weight degradation at various water-cuts. It is clearly seen that samples immersed in dried IRM-903 oil and Balmoral Crude oil (from Norway offshore platform) do not undergo the significant amount of molecular weight loss encountered in more aqueous conditions. Polar amide-bond linkages are stabilized in non-polar conditions, whereas even a small percentage of water present proves to be detrimental to the molecular weight of nylon.

Plots of molecular weight versus temperature can yield significant rate kinetics data. Assuming a first order rate dependence, the following equation is created,

$$MW(t) = MW_o e^{-kt} \qquad [4.1]$$

where $MW(t)$ is the molecular weight at time t, MW_o is the initial molecular weight, and k is the degradation rate constant specific to that certain temperature. k can be determined by plotting the natural logarithm of molecular weight versus day at various temperatures. **Fig. 4.7** shows that the data are well-represented by first order kinetics. Another useful equation that can be employed at

this stage is the Arrhenius Equation,

$$k = Ae^{\frac{-E_a}{RT}} \qquad [4.2]$$

where A is called the pre-exponential factor, E_a is the activation energy in J/mol, R is the ideal gas constant (8.314 J K^{-1} mol^{-1}), and T is the temperature (in Kelvin). With the k values from the five different temperatures obtained from **Fig. 4.7**, a kinetic fit can be made by plotting *ln k vs. 1/T*. This plot is seen in **Fig. 4.8**. From the slope of -7.1 K^{-1}, an activation energy of 59.1 kJ/mol and a pre-exponential factor of 2.33 x 10^6 $days^{-1}$ are determined. These values are comparable to the values obtained from studies of the previous phases, where E_a = *60.2 kJ/mol* and $A = 3.27 \times 10^6$ $days^{-1}$ (see **Ref. 3**).

PVDF

PVDF is an important inner fluid barrier for use in the advanced high temperature pipes (see Chapter 2). As such, it is important to understand and examine the stability of PVDF in harsh chemical environments typically

encountered in oil platforms.

In this study, PVDF is examined in a variety of conditions mimicking the use of solvents and treatment agents in an oil pipe. As mentioned previously in Chapter 1, two types of PVDF (Wellstream and Coflexip) with different plasticizer contents are used for testing. **Table 4.4** gives a list of the types of environments PVDF is subjected to.

For the testing of corrosion inhibitors, strips of PVDF are added to 100% Aniline, 90% Ethylene glycol (EG)/10% Tetraethylammonium chloride (TEAC), EG/1000ppm TEAC, and Water/1000ppm Aniline.

The latter two experiments have just been started and early molecular weight data so far indicate much slower degradation than their higher concentration counterparts seen in **Table 4.5**. The plots for *MW vs. Days and Log MW vs. Days* for both types of PVDF in the four environments shown in the table are given in **Figs. 4.9-12.**

The first two conditions have been recently completed, and the dielectric data from those two studies were averaged, merged, and plotted in **Figs. 4.13-16.** From the values of $\epsilon'' \times \omega$, it can be seen that the ionic mobility in the PVDF increases as the material ages in

both conditions. This points to infiltration of the solvent and degradation.

The rate of ion pickup by the polymer can be noted in plots of ϵ'' at one chosen frequency. Plots of ϵ'' at 1 kHz for both types of PVDF in 100% Aniline and in EG/10% TEAC are shown in **Figs. 4.17 & 4.18**. Both figures show that Wellstream PVDF seems to allow ionic diffusion more readily than Coflexip both initially and towards the end of the study. In addition, the infiltration of EG into PVDF is to be much greater than aniline, though ionic mobility in the Aniline condition increases dramatically at later days.

Weight loss measurements at the same time revealed an interesting finding (**Tables 4.6 & 4.7, Figs. 4.19 & 4.20**). In 130°C air, PVDF loses weight as expected due to plasticizer content being driven off. Weight loss is seen in the EG/10% TEAC condition as well, though not as much as in the air. There is a slight weight gain, however, in the PVDF in the 100% Aniline. This may be due to a greater uptake of Aniline with less plasticizer loss, though the overall scheme of degradation in Aniline is unclear at this point.

Other chemicals used include 100% Ethylene glycol to

simulate dehydration agent and 60% Water/40% Ammonium bisulfate for scale inhibition. Both of these test conditions are at their early stages and have not yet yielded any results.

Besides tests in these chemical conditions, PVDF FDEMS sensors have also been tested in 130°C air (**Fig. 4.21** and **4.22**) and 130°C 95% IRM-903 oil/5% water (**Fig. 4.23** and **4.24**). These plots show fairly flat frequencies after an initial time, which is attributed to the stability of PVDF. **Fig. 4.25** is a plot of the weight loss of PVDF in the 130°C 95% oil, and it shows a slow rate of loss after the initial plasticizer is driven off.

In the 95% oil environment there also includes a Coflexip sensor that was deplasticized in 130°C air for a period of two months, and a FDEMS run of this material after several weeks is seen in **Fig. 4.26**.

The continued low dielectric readings of **Fig. 4.26** show that replasticization by the environment of the aged material is not occurring. This could be due to higher density of the PVDF when it was first deplasticized at 130°C, which led to a high crystallinity that can inhibit ion diffusion. Because PVDF is extremely stable to its

environments, a longer term of study is necessary to gather more useful degradation data.

Chemflake

The apparatus for testing of Chemflake vinyl ester is set up as follows. Eight steel plates with dimensions of approximately 65mm x 35mm x 1.5mm were cleaned and mildly sanded. Four glass FDEMS sensors were made with teflon coated copper leads and lightly taped onto four of the plates. A batch of Chemflake material was prepared using 69.7g of Chemflake Base, 0.91g of Norpol Accelerator 9802, 0.29g of Norpol DMA 9826, and 1.25g of Norpol Catalyst. After thorough stirring the mixture was rapidly applied to one side of all eight plates, covering the sensors on four of the plates.

At the same time, a small portion of the Chemflake mixture was set aside to be tested in the DSC and by the Barcol Hardness meter periodically. The results of the DSC scans are shown in **Figs. 4.27-33.** The heat of reaction and change in hardness during cure are shown in **Tables 4.8** and **4.9.** The FDEMS data during the cure of the material can be plotted with α, the degree of cure, seen

in **Fig. 4.34**, as well as a direct correlation of both FDEMS and alpha, seen in **Fig. 4.35**. Similar plots can be made for the measured Barcol hardness during cure (**Figs. 4.36** and **4.37**). Such correlations indicate the usefulness and the need for comparing data collected on various instrumentations.

After the first batch of Chemflake was cured at room temperature for over 70 hours, another batch was prepared. This portion contained 69.49g of the Base, 0.90g of Norpol Accelerator 9802, 0.28g of Norpol DMA 9826, and 1.24g of Norpol Catalyst. The mixture was carefully and evenly poured over the previously untreated backside of the steel plates. After the plates were entirely covered, they were allowed to sit at room temperature for 24 hours. To ensure that the material is fully cured, the eight plates (four with sensors and four without) were allowed to sit at room temperature for two weeks while the heating environment was set up.

After weighing and measuring the thickness of the four sensorless plates, or coupons, all eight plates were introduced into the acid bath apparatus. The apparatus is a glass desiccator placed in a water bath with a temperature fixed at 45°C using a Dyna-Sense temperature

controller with constant stirring. Approximately one liter of concentrated hydrochloric acid was poured into the desiccator. An empty beaker was placed in the acid bath, weighed down by glass beads. Four plates (two sensors and two coupons) were put into the beaker to simulate acid vapor conditions while the other four were placed in the desiccator directly in contact with the acid.

Continuous FDEMS data acquisition was made prior to and after the introduction of the sensor into the acid environment. Measurements were subsequently taken periodically, and the data were all merged after eleven days. Plots of a sensor plate in vapor and one in the liquid (HCl) are shown in **Figs 4.38** and **4.39**. As the Chemflake sits in the acid bath, some of the polymer leeches out into the acid as indicated by a darkening of the liquid and the coating, as well as the weight change (**Table 4.10** and **Fig. 4.40**) and hardness (**Fig. 4.41**).

Figure 4.1 FDEMS of Nylon-11 sensor in 95°C 95% IRM-903 oil/5% Water with CO_2, log ϵ'

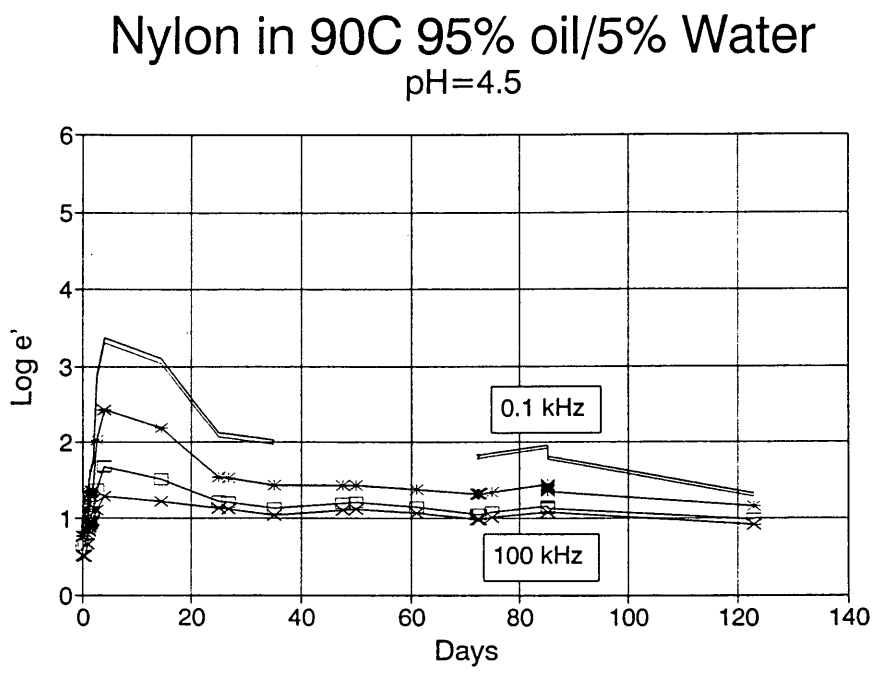

Figure 4.2 FDEMS of Nylon-11 sensor in 95°C 95% IRM-903 oil/5% Water with CO_2, log ϵ'' x ω

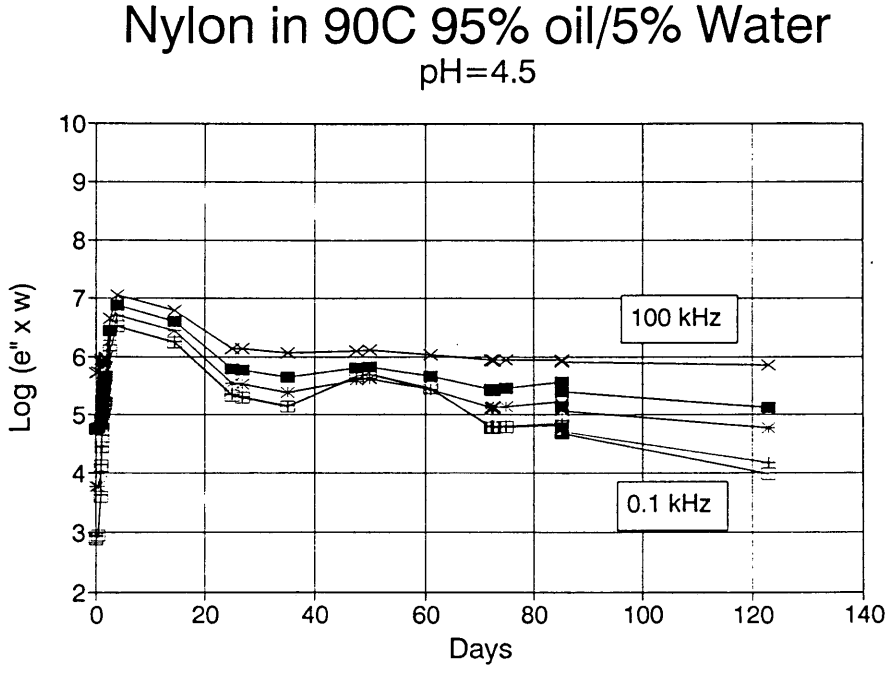

Table 4.1 Nylon-11 testing environments

Temperature	pH	Environment
105°C	-	100% ASTM oil (DRY)
	-	100% Balmoral Crude (30-50% H_2O)
	-	Balmoral Crude (DRY)
	4.5	95% ASTM oil/5% H_2O
	6.0	95% ASTM oil/5% Buffer
	4.5	5% ASTM oil/95% H_2O
	4.5	100% H_2O
	6.0	100% Buffer
	7	100% H_2O
130°C	4.5	5% ASTM oil/95% H_2O
120°C	4.5	95% ASTM oil/5% H_2O
	6.0	95% ASTM oil/5% Buffer
	7	100% H_2O
90°C	4.5	95% ASTM oil/5% H_2O
	6.0	95% ASTM oil/5% Buffer
	4.5	5% ASTM oil/95% H_2O
	6.0	100% Buffer
	7	100% H_2O
70°C	4.5	95% ASTM oil/5% H_2O
	6.0	95% ASTM oil/5% Buffer
	4.5	5% ASTM oil/95% H_2O
	7	100% H_2O

Table 4.2 Molecular Weight of Nylon-11 in various Environments at 105°C

Day	100% IRM oil 105C	Balmoral oil 105C	Dry Balmoral 105C	95% IRM oil 105C*	95% IRM oil 105C**	5% IRM oil 105C*	100% Water 105C*	100% Water 105C**	100% Water 105C
0	52300	52300	52300	52300	52300	52300	52300	52300	52300
4						44000			
5	57800								
7					44000	39800	47800	51000	
14	41400	59200	54770	36500		35000			37920
21	54200						37000		
24						30700			
25								34530	
27			56000						
28	49700	46200							
29				33800					
35						30880	30160		29210
36		48400	48410						
49					28460			19210	
50				29000					
63	47320	42900							
66									21360
75							22060		
96				19200					
100									13830
109							9700		
134	33310								
215		22000							

* - denotes charged with carbon dioxide

** - denotes buffered at pH = 6

IRM stands for Industry Research Materials

Table 4.3 Molecular Weight of Nylon-11 in various Environments at 70°C, 90°C, 120°C, and 130°C

Day	100% Water 70C	95% IRM oil 90C*	95% IRM oil 90C**	100% Water 120C	95% IRM oil 120C**	5% IRM oil 130C*
0	52300	52300	52300	52300	52300	52300
4						39500
7	51010		50300		30630	
8						20500
16	49860			24300		
20						17100
25		38960				
30						14300
49					12530	
53	47290					
57		29400				

* - denotes charged with carbon dioxide

** - denotes buffered at pH = 6

Figure 4.3 Molecular Weight vs. Days of Nylon-11 at 105°C with pH = 4.5, 6.0, and 7

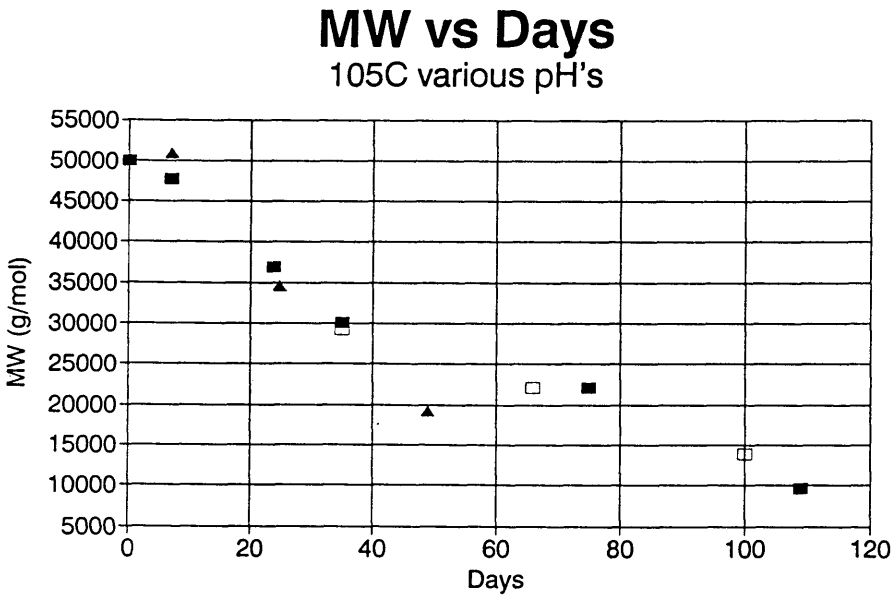

Figure 4.4 Log Molecular Weight vs. Days of Nylon-11 at 105°C with pH = 4.5, 6.0, and 7

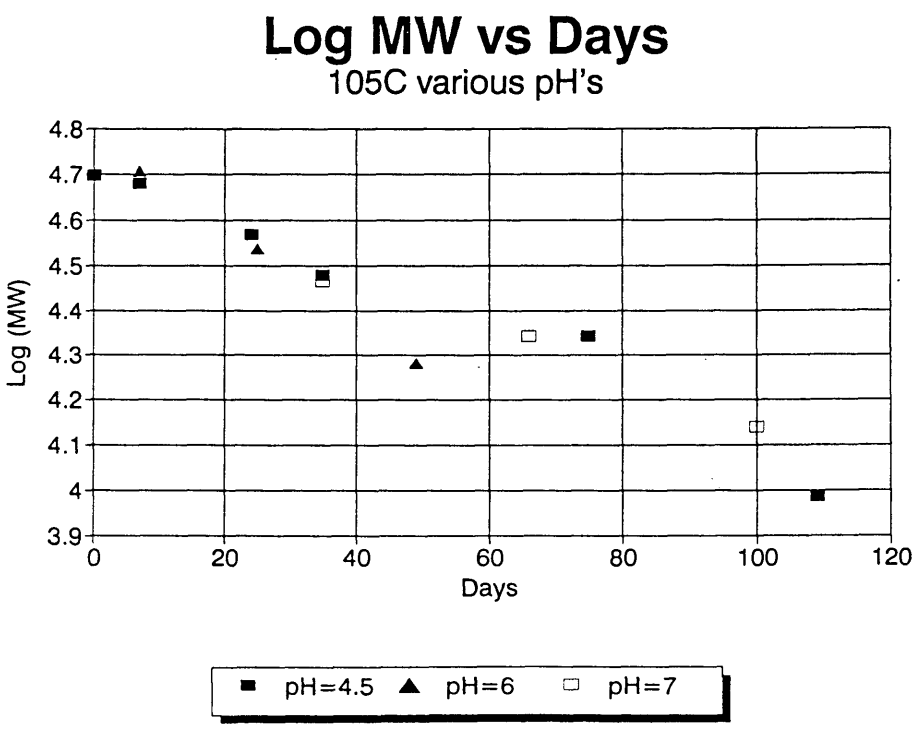

Figure 4.5 Molecular Weight vs. Days of Nylon-11 at 105°C and pH = 4.5 at various water-cuts

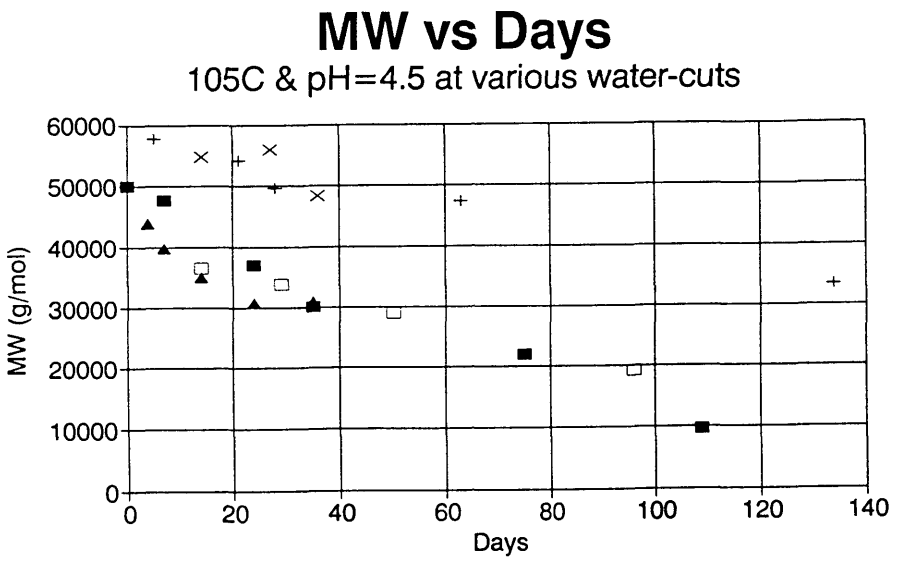

Figure 4.6 Log Molecular Weight vs. Days of Nylon-11 at 105°C and pH = 4.5 at various water-cuts

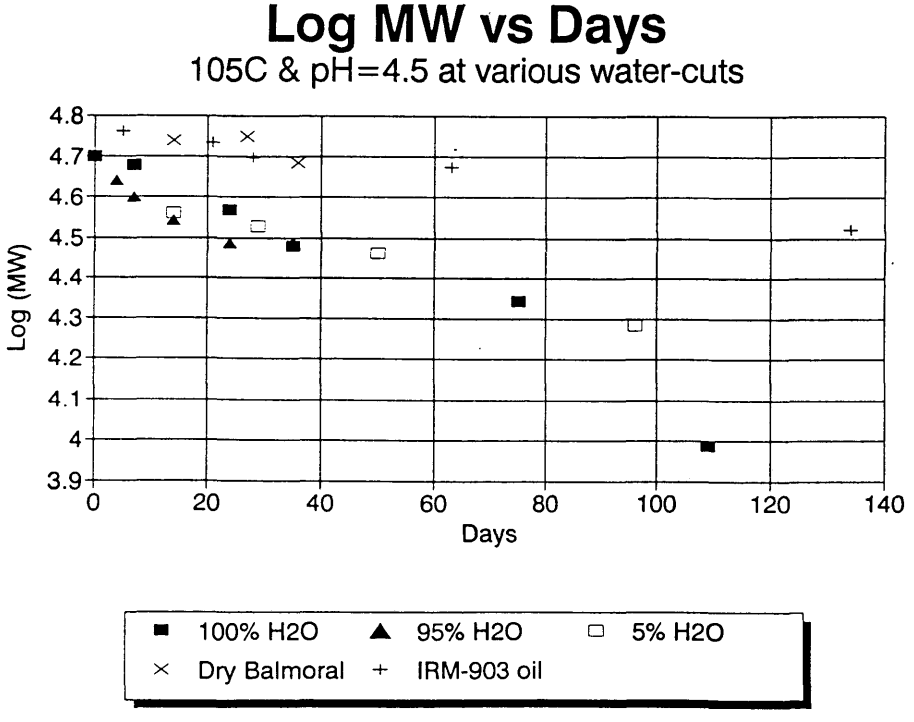

Figure 4.7 Ln Molecular Weight vs. Days of Nylon-11 at 70°C, 90°C, 105°C, 120°C and 130°C

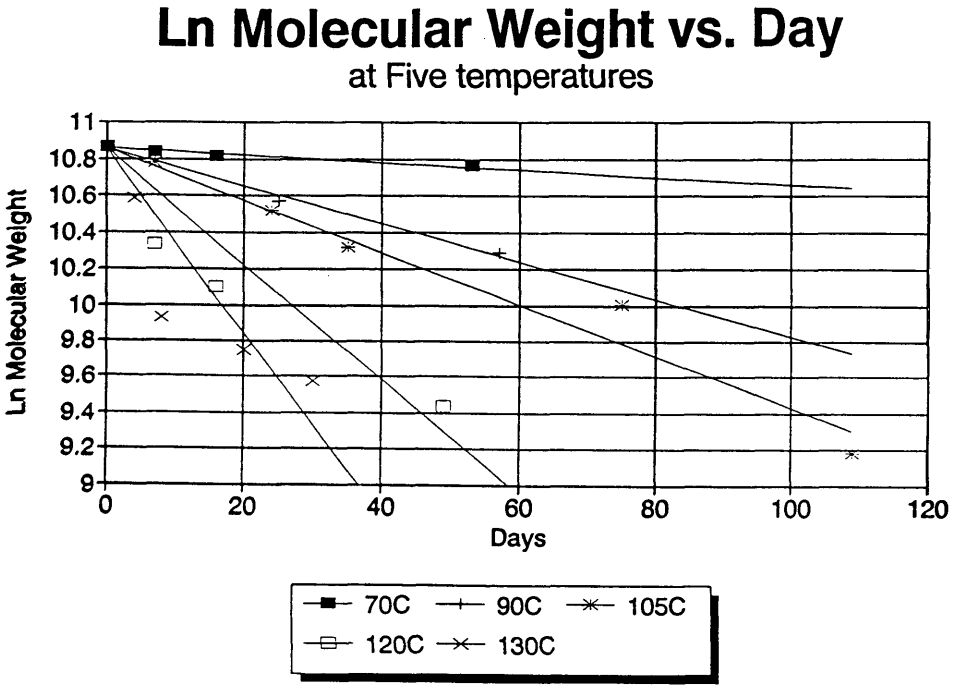

Figure 4.8 Ln *k* vs. 1/T of Nylon-11 for Arrhenius Fit at 70°C, 90°C, 105°C, 120°C and 130°C

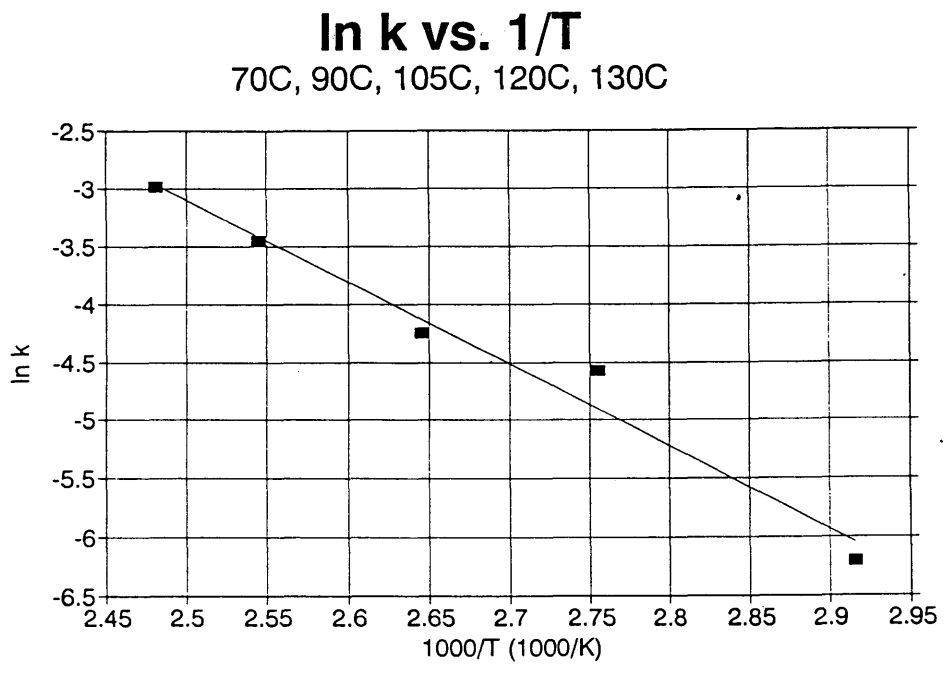

Table 4.4 PVDF testing environments, at 130°C

- 95% IRM-903 oil/5% H_2O, pH = 4.5
- 95% IRM-903 oil/5% H_2O, pH = 4.5, deplasticized
- Air Oven
- 100% Aniline
- 100% Ethylene glycol
- Ethylene glycol & 10% (by wt.) Tetraethylammonium chloride
- Ethylene glycol & 1000 ppm Tetraethylammonium chloride
- Water & 1000 ppm Tetraethylammonium chloride
- Water & 1000 ppm Aniline
- 40% Water/60% Ammonium bisulfate, $(NH_4)HSO_4$
- Water & 1000 ppm Ammonium bisulfate

Table 4.5 Calculated Molecular Weight of PVDF in Various Environments

Wellstream				
Day	Air 130C	95% IRM oil 130C	100% Aniline 130C	EG & 10% TEAC 130C
0	620000	620000	620000	620000
1	772000		784000	674000
2	529000		775000	
4			762000	
5		718000		
8			729000	514000
14	705000			
16				510000
24			345000	
26		691000		
28	671000			
39				482000
46			336000	
53				410000
61			234000	
73		694000		
98				
107		713000		
128				329000
136				
170	658000			

Coflexip				
Day	Air 130C	95% IRM oil 130C	100% Aniline 130C	EG & 10% TEAC 130C
0	594000	594000	594000	594000
1			732000	649000
2			678000	
4			678000	
5		636000		
8			636000	
14				
16				
24				
26		678000		
28	678000			
39				708000
46			555000	
53				531000
61			461000	
73				
98		688000		
107				
128				404000
136			LOW	
170				

EG = Ethylene Glycol TEAC = Tetraethylammonium chloride

Figure 4.9 Molecular Weight vs. Days of Wellstream PVDF in various environments

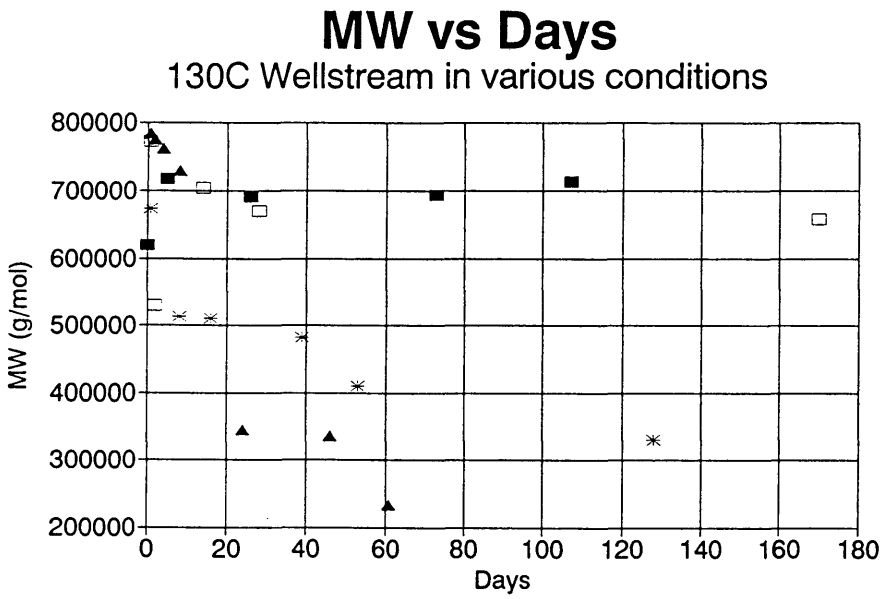

Figure 4.10 Log Molecular Weight vs. Days of Wellstream PVDF in various environments

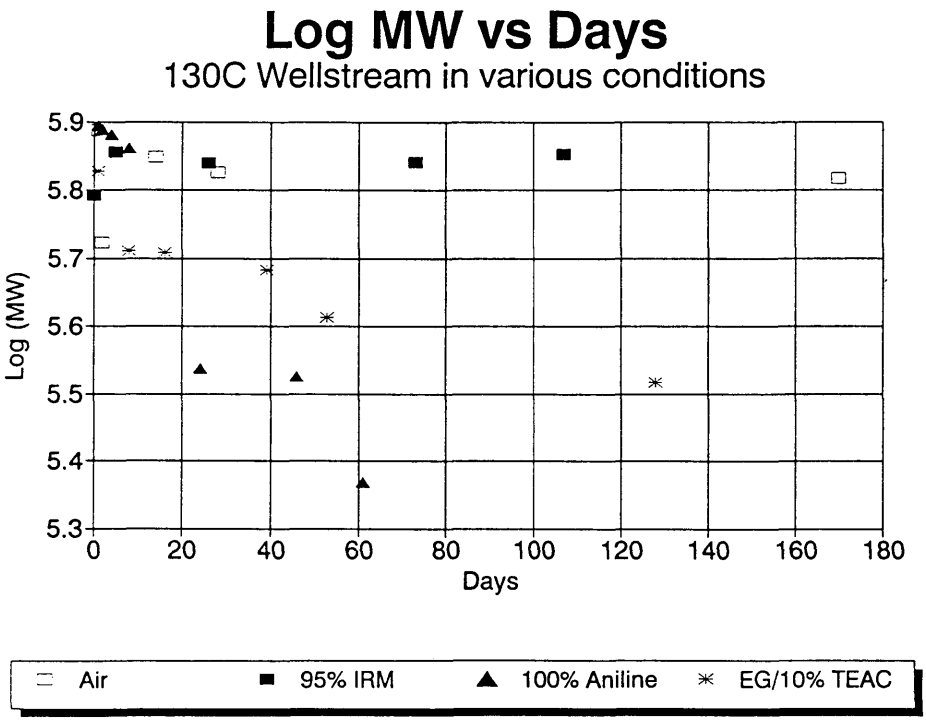

Figure 4.11 Molecular Weight vs. Days of Coflexip PVDF in various environments

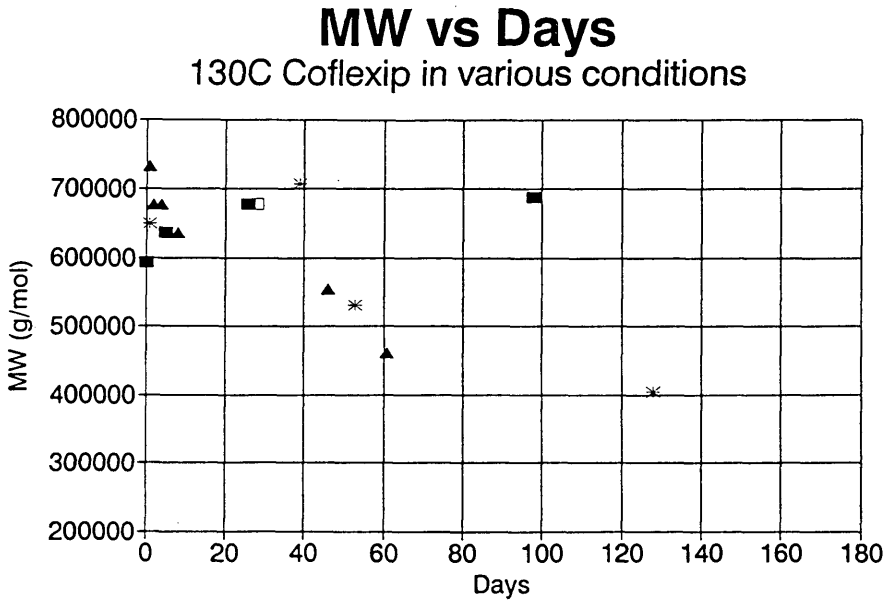

Figure 4.12 Log Molecular Weight vs. Days of Coflexip PVDF in various environments

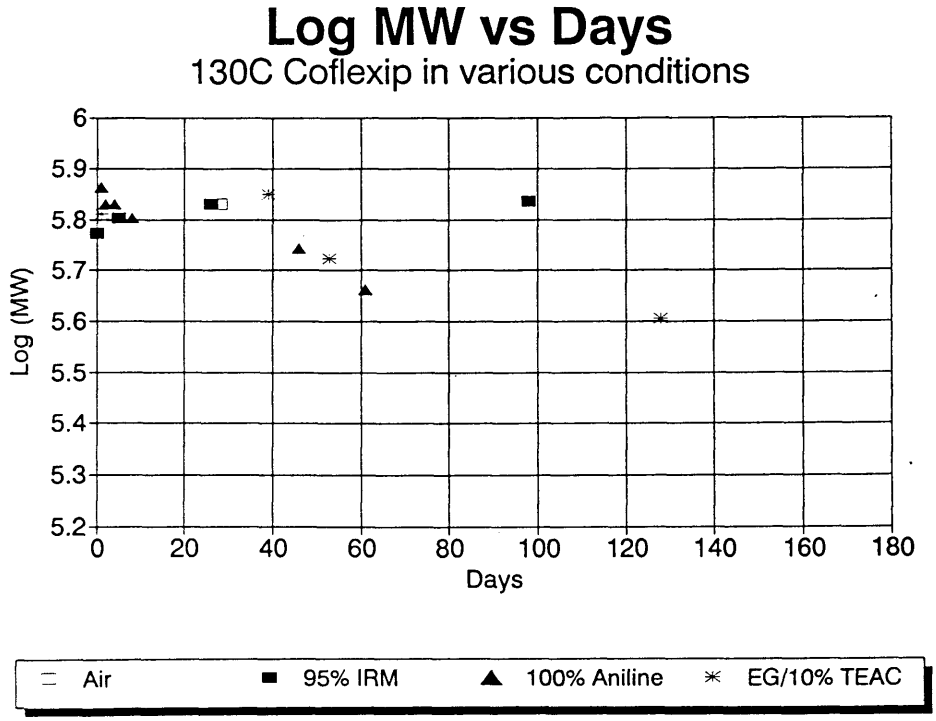

Figure 4.13 FDEMS plot of Wellstream PVDF in 130°C 100% Aniline

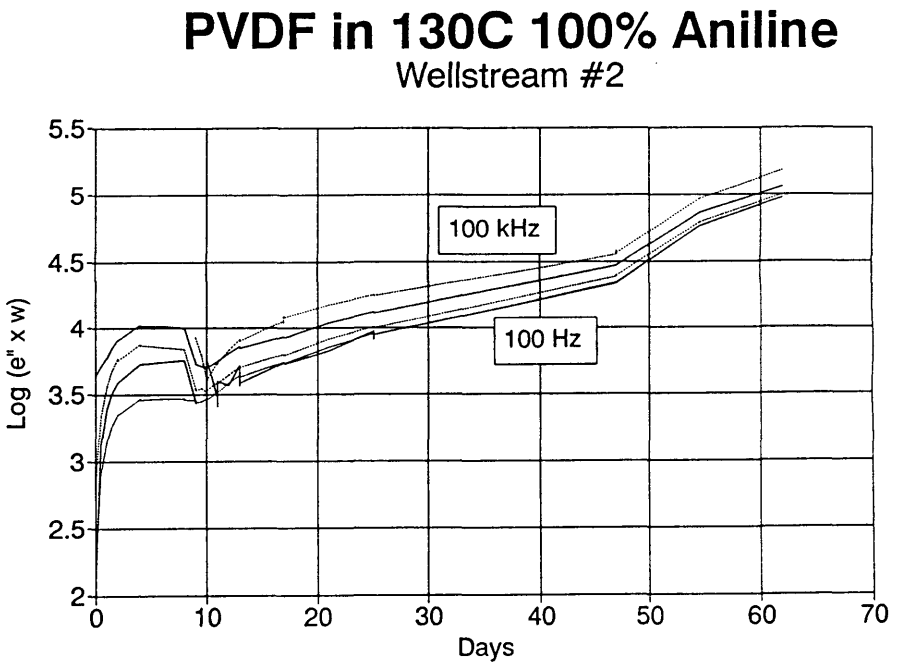

Figure 4.14 FDEMS plot of Coflexip PVDF in 130°C 100% Aniline

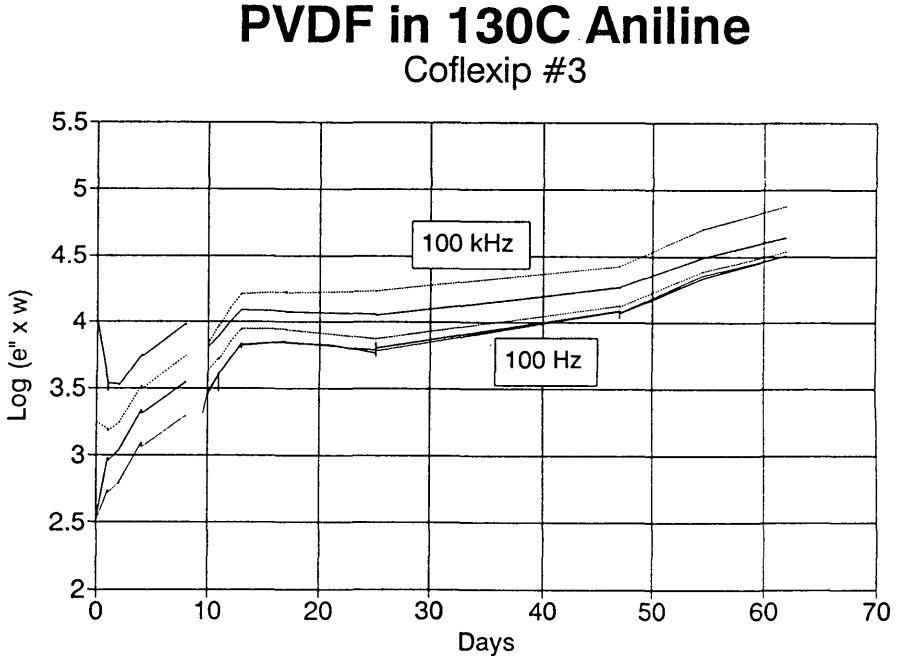

Figure 4.15 FDEMS plot of Wellstream PVDF in 130°C Ethylene glycol and 10% Tetraethylammonium chloride

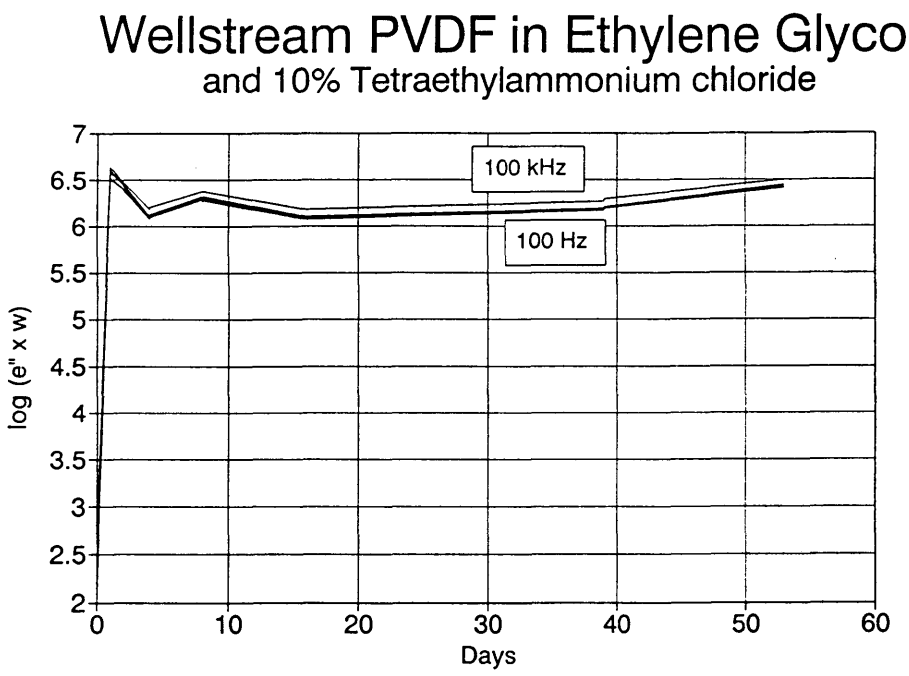

Figure 4.16 FDEMS plot of Coflexip PVDF in 130°C Ethylene glycol and 10% Tetraethylammonium chloride

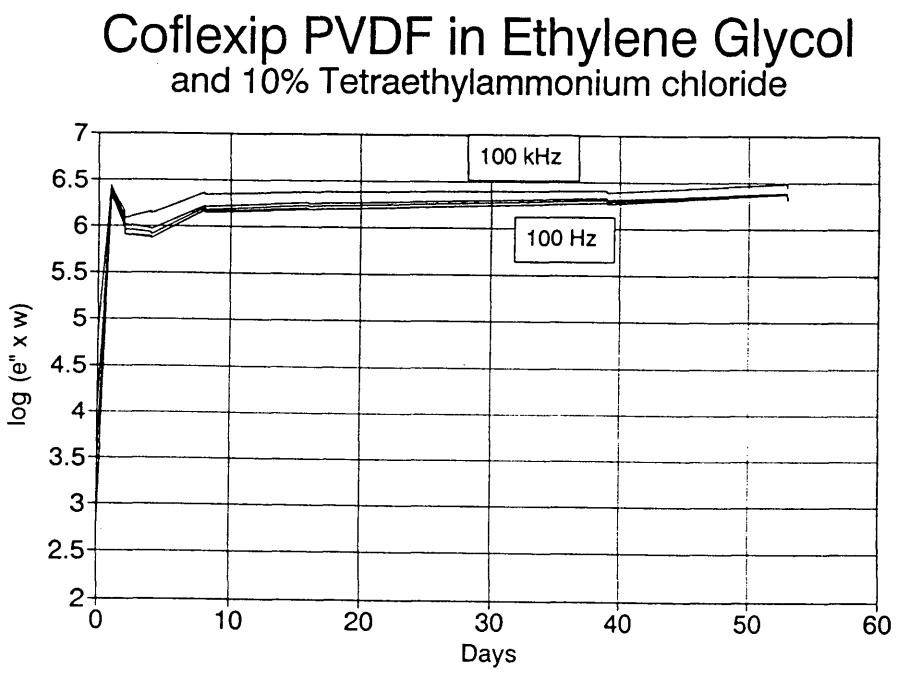

Figure 4.17 ε" vs Days of PVDF in 130°C Aniline, 1 kHz

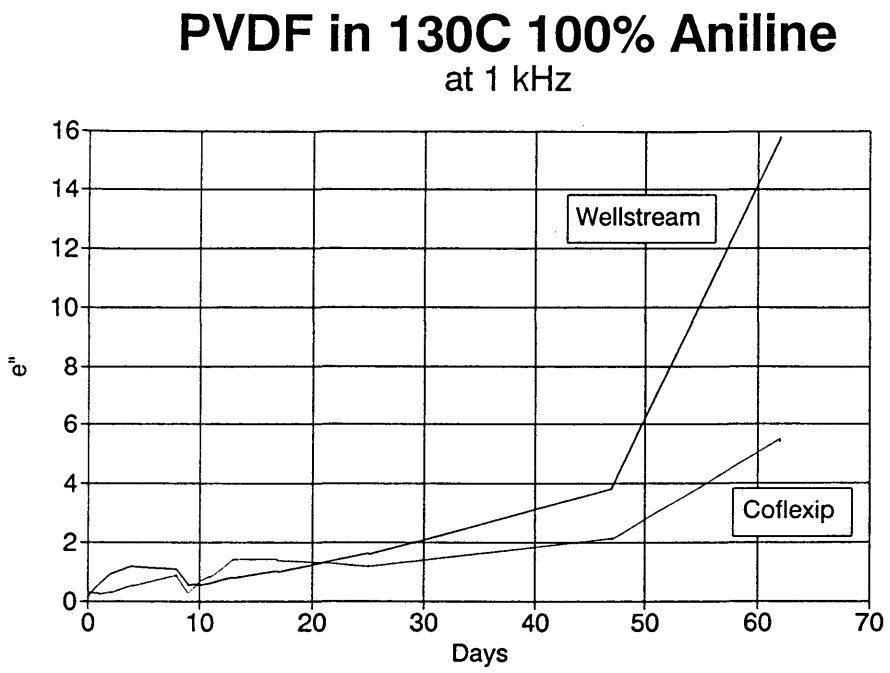

Figure 4.18 ε" vs Days of PVDF in 130°C Ethylene glycol/10% Tetraethyl-ammonium chloride, 1 kHz

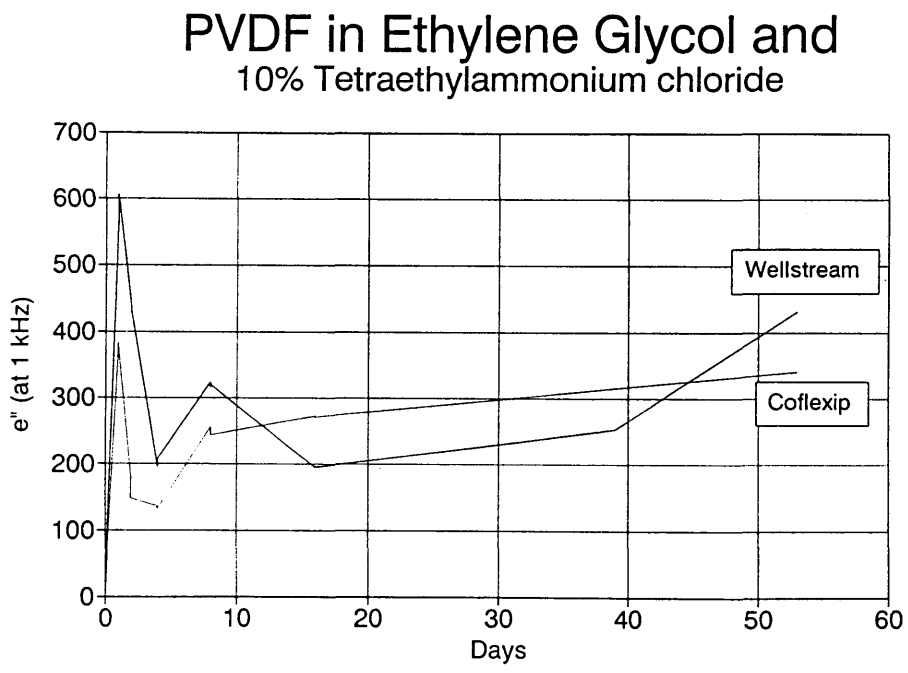

Table 4.6 Weight loss data of Wellstream PVDF in 130°C Air, 100% Aniline, and Ethylene glycol/10% TEAC

Wellstream PVDF Weight Loss Data						
	Mass of Pieces (g)			Percent Weight Remaining		
Day #	Aniline	Glycol	Air	Aniline	Glycol	Air
0	3.4366	3.2714	3.2697	100	100	100
1	3.6198	3.1861	3.0847	105.3309	97.39255	94.34199
2	3.6227	3.1758	3.0415	105.411	97.06927	92.94153
4	3.6460	3.1672	3.0022	106.0541	96.79848	91.6494
8	3.6443	3.1501	2.9730	106.0075	96.25857	90.67678
16	3.6445	3.1377	2.9483	106.013	95.86493	89.84597
39	3.6340	3.1295	2.9350	105.7249	95.60359	89.39486
53	3.6594	3.1230	2.9336	106.4238	95.39589	89.34716

Table 4.7 Weight loss data of Coflexip PVDF in 130°C Air, 100% Aniline, and Ethylene glycol/10% TEAC

Coflexip PVDF Weight Loss Data						
	Mass of Pieces (g)			Percent Weight Remaining		
Day #	Aniline	Glycol	Air	Aniline	Glycol	Air
0	4.1623	5.2067	2.7176	100	100	100
1	4.4225	5.1410	2.6198	106.2514	98.73816	96.40124
2	4.4910	5.1187	2.5776	107.8002	98.3044	94.79043
4	4.4376	5.0910	2.5321	106.6112	97.76324	93.02522
8	4.4248	5.0388	2.4846	106.3228	96.7379	91.14931
16	4.4278	5.0083	2.4458	106.3906	96.1326	89.58769
39	4.4168	4.9960	2.4322	106.1421	95.88701	89.03163
53	4.4591	4.9909	2.4313	107.0998	95.78493	88.99463

Figure 4.19 Weight loss vs Days of Wellstream PVDF in 130°C air, 100% Aniline, and EG/10% TEAC

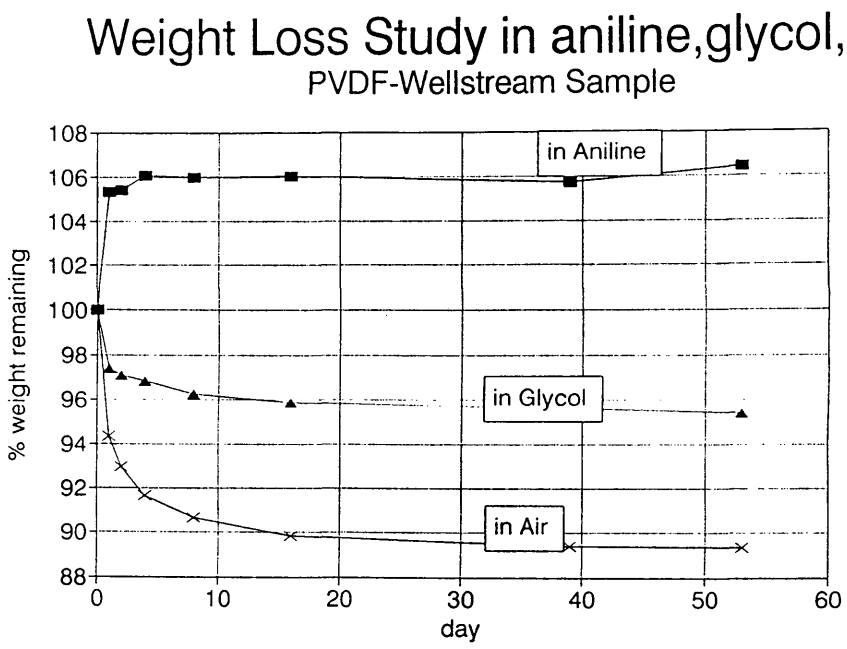

Figure 4.20 Weight loss vs Days of Coflexip PVDF in 130°C air, 100% Aniline, and EG/10% TEAC

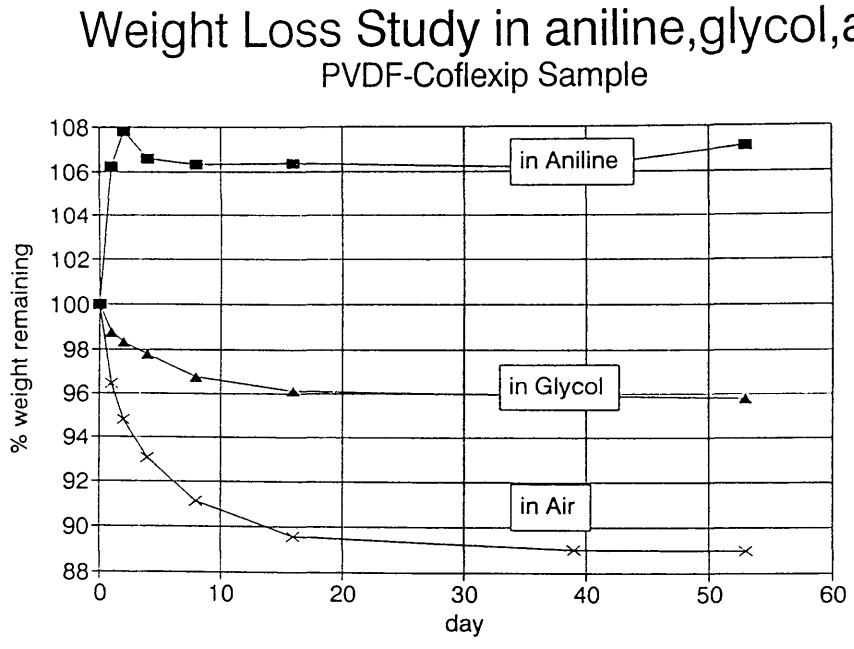

Figure 4.21 FDEMS plot of Wellstream PVDF in 130°C Air

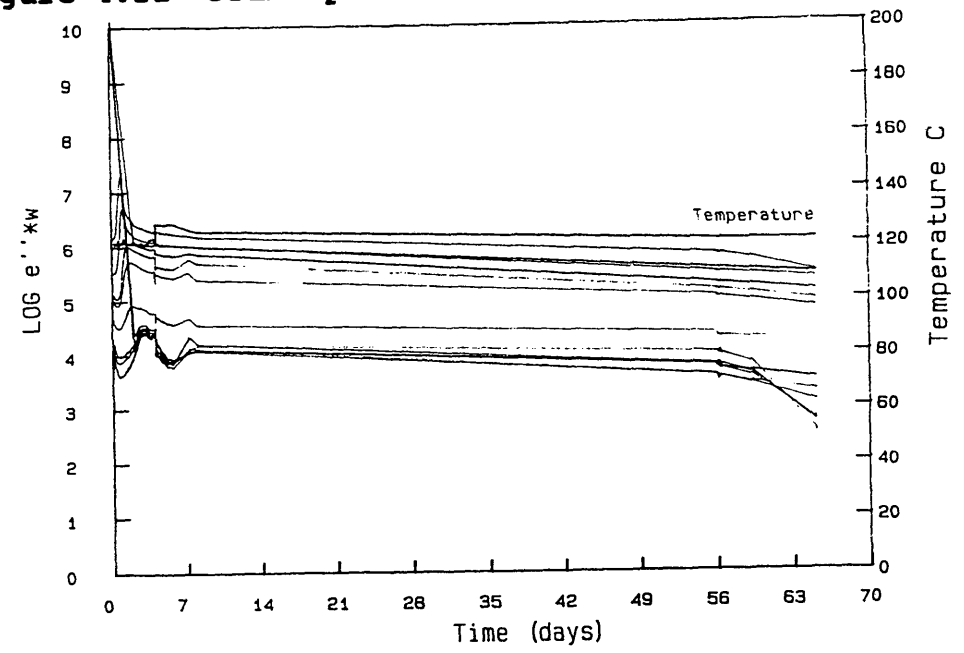

Figure 4.22 FDEMS plot of Coflexip PVDF in 130°C Air

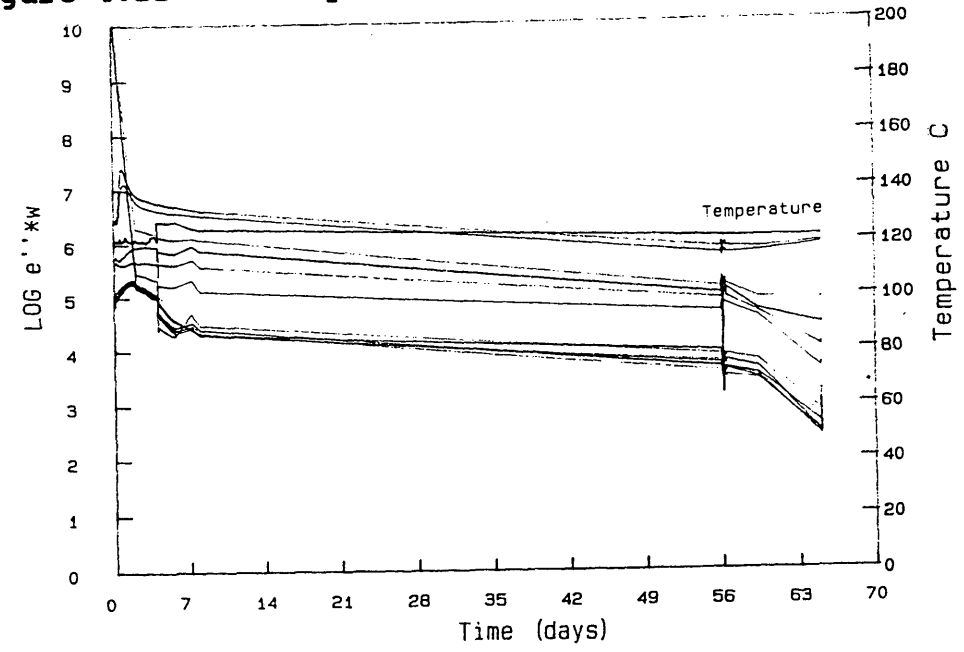

Figure 4.23 FDEMS plot of Wellstream PVDF in 130°C 95% IRM-903 oil/5% Water (WR)

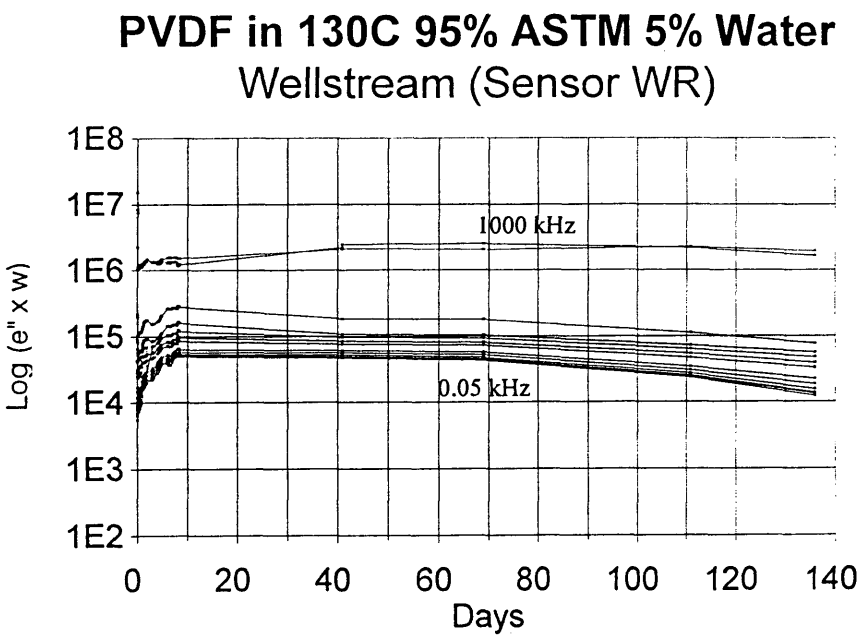

Figure 4.24 FDEMS plot of Wellstream PVDF in 130°C 95% IRM-903 oil/5% Water (WL)

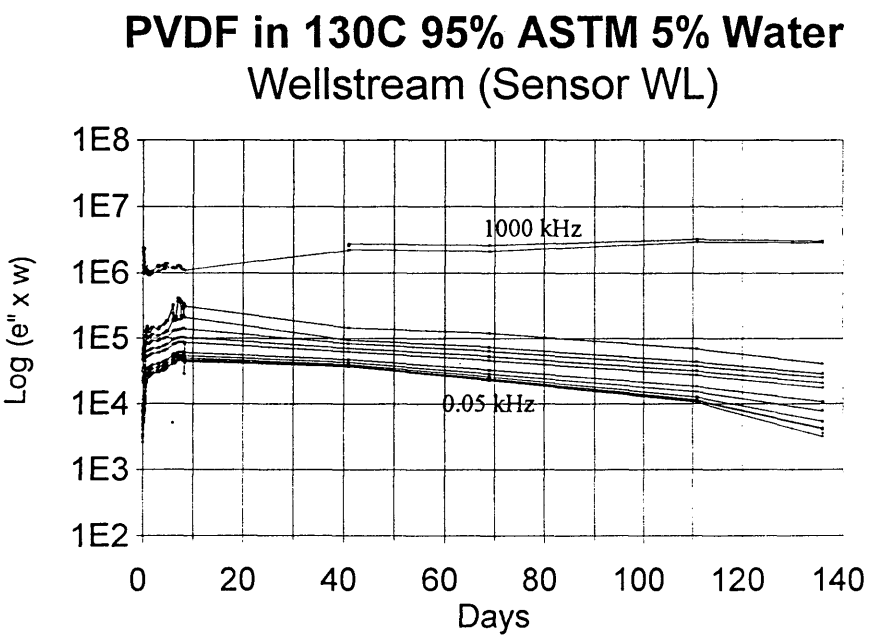

Figure 4.25 Weight loss vs Days of PVDF in 130°C 95% IRM oil/5% Water with CO_2

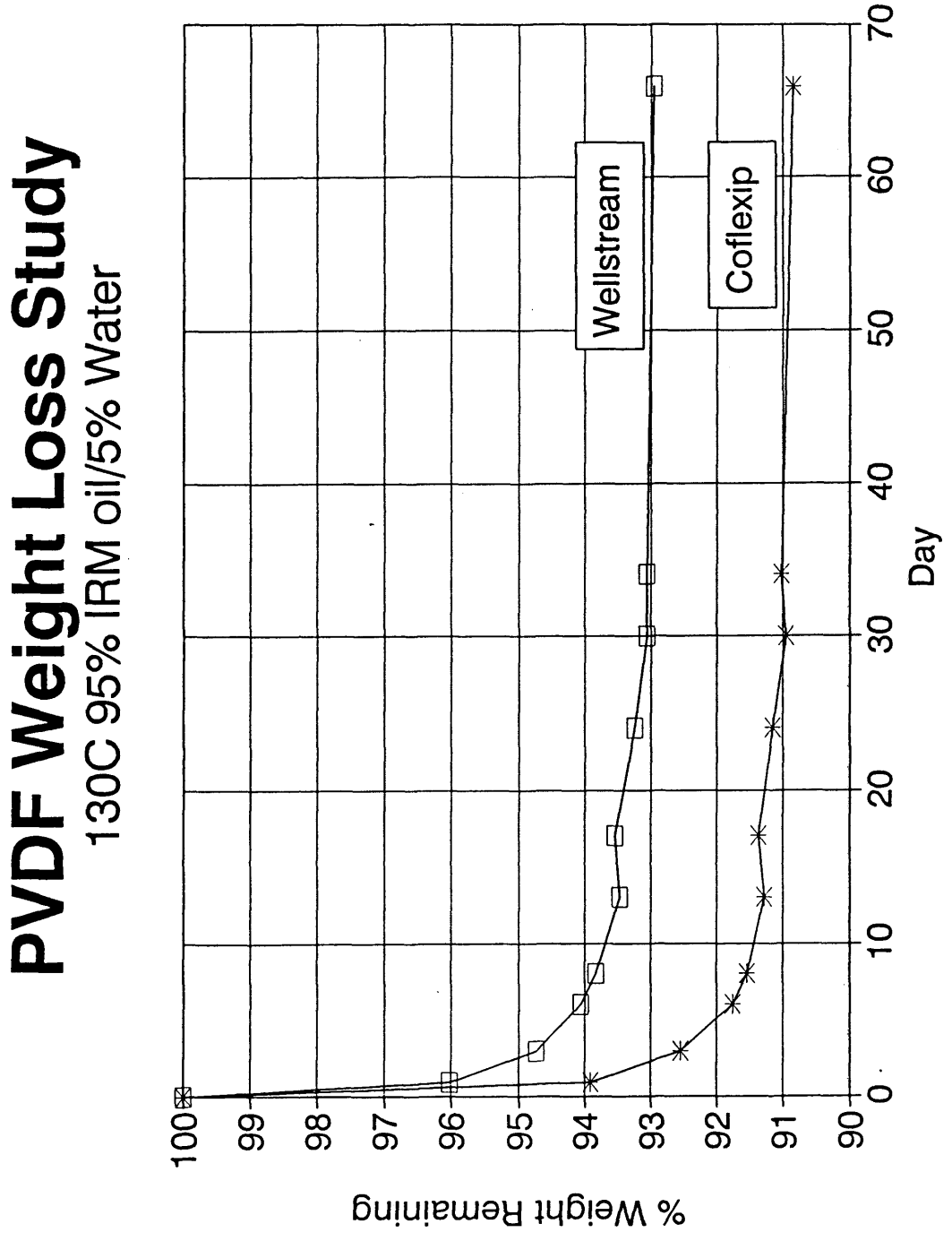

Figure 4.26 FDEMS plot of deplasticized Coflexip PVDF in 130°C 95% IRM oil/5% Water with CO_2, 11 days in the mixture

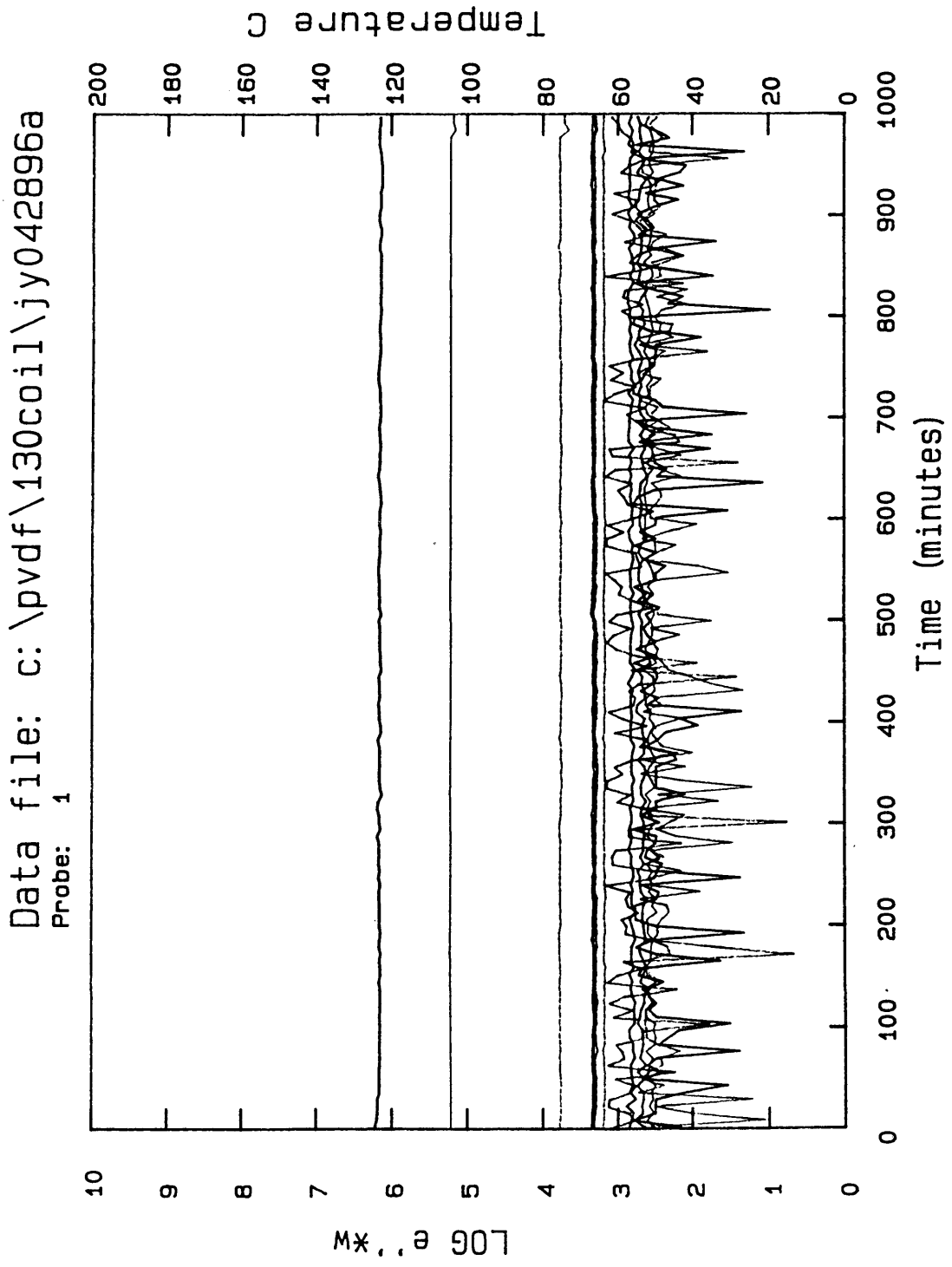

Figure 4.27 DSC plot of Chemflake cure at 0 hours

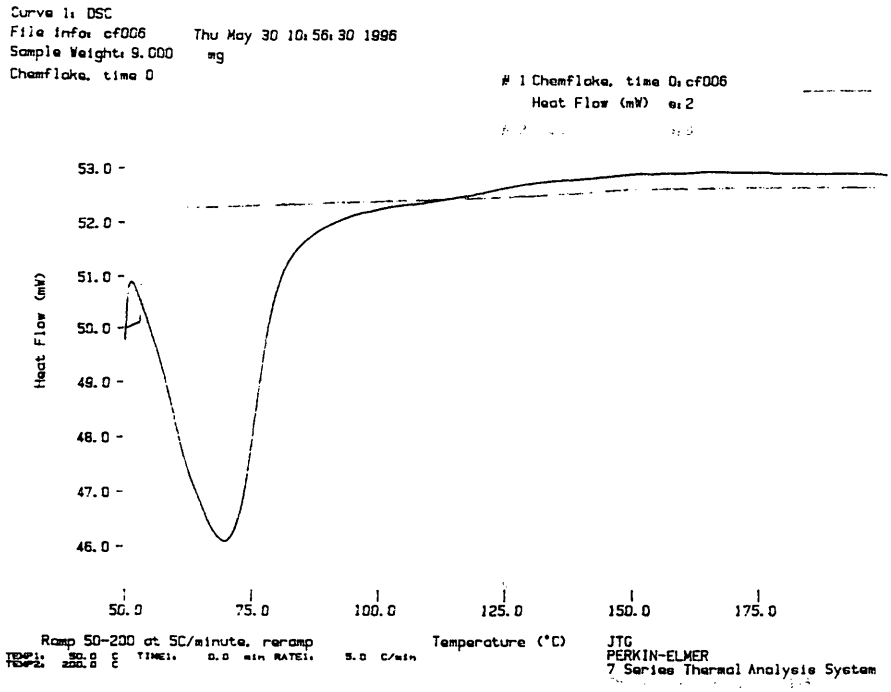

Figure 4.28 DSC plot of Chemflake cure at 1 hours

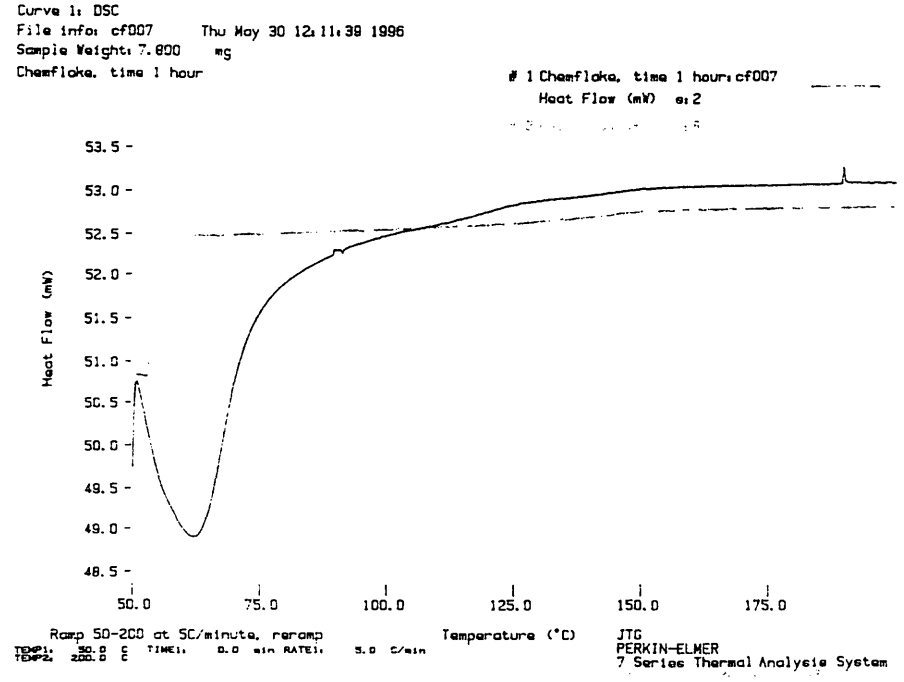

Figure 4.29 DSC plot of Chemflake cure at 2 hours

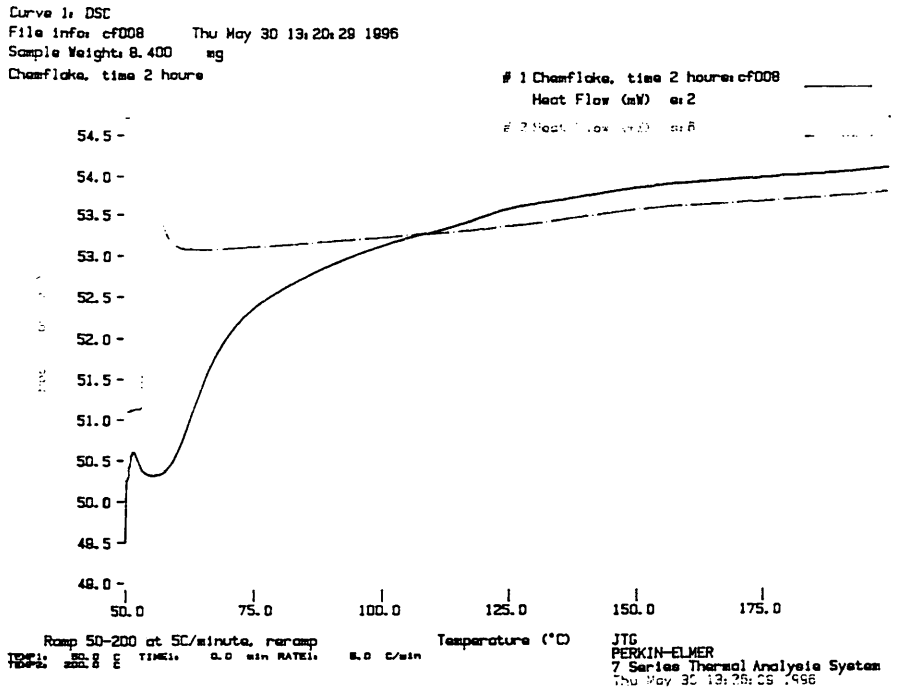

Figure 4.30 DSC plot of Chemflake cure at 4 hours

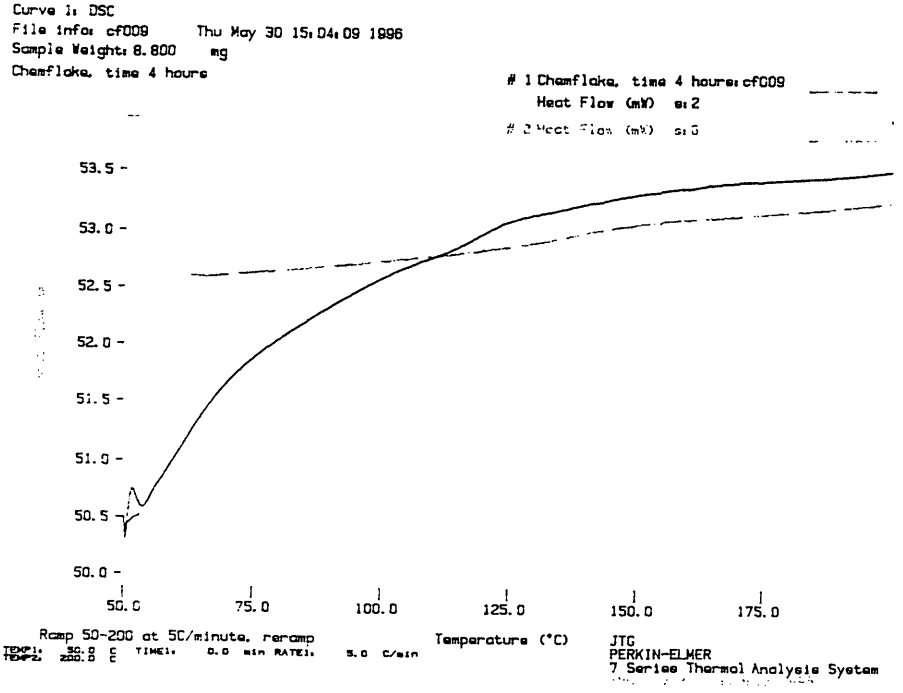

Figure 4.31 DSC plot of Chemflake cure at 8 hours

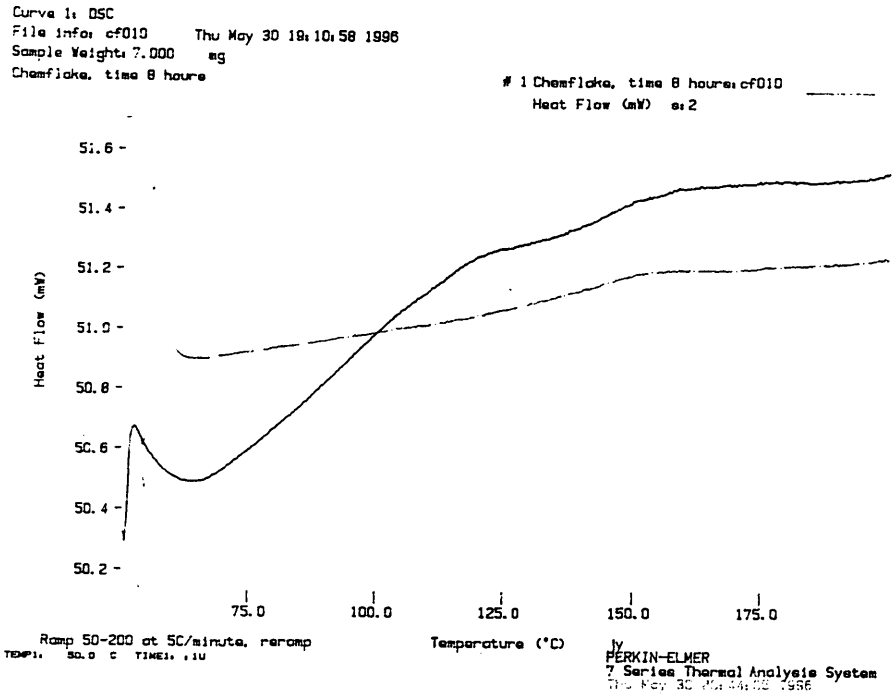

Figure 4.32 DSC plot of Chemflake cure at 24 hours

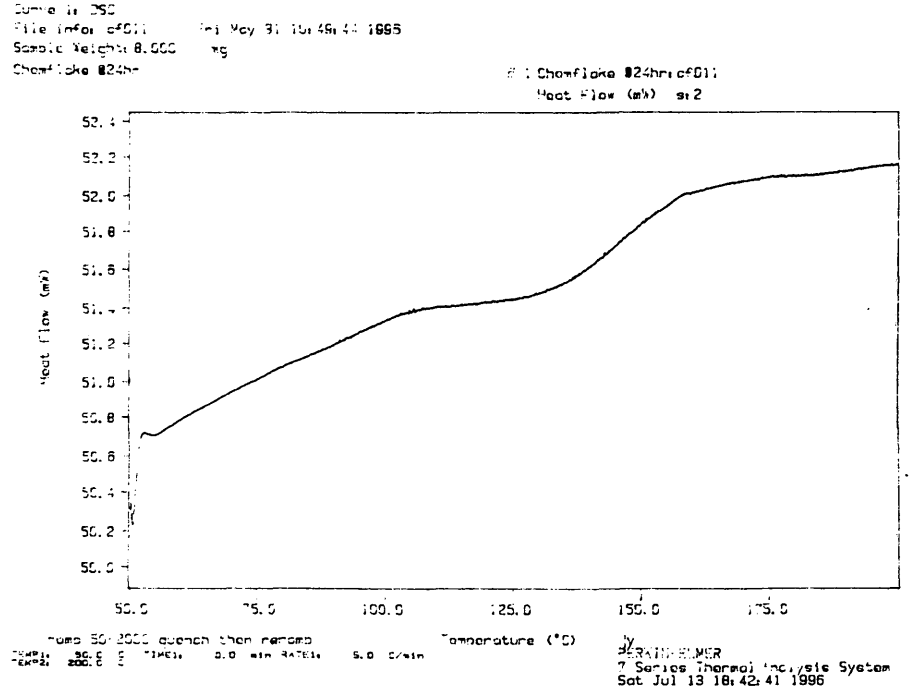

Figure 4.33 DSC plot of Chemflake cure at 48 hours

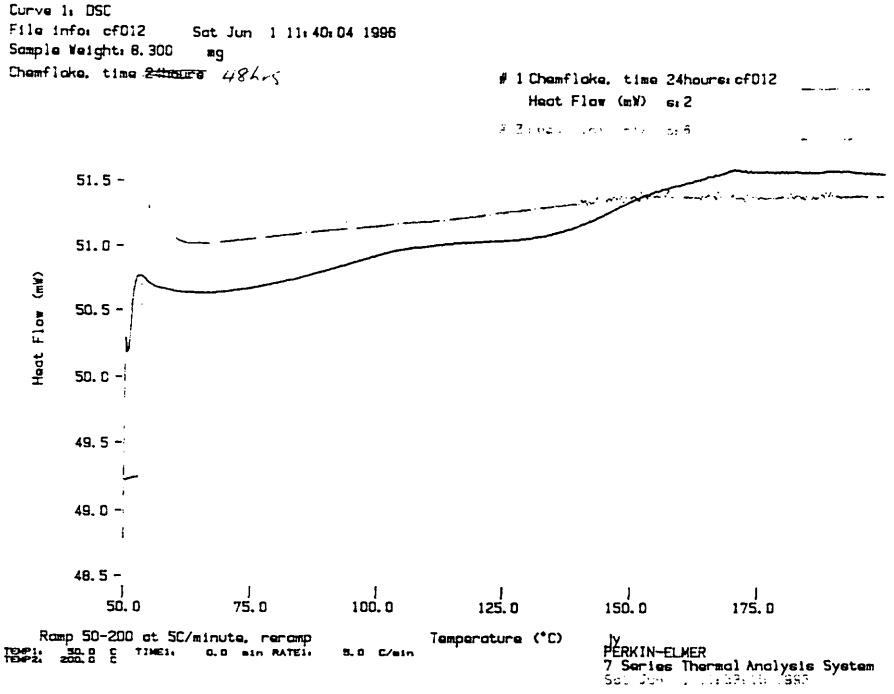

Table 4.8 Calculated ΔH_{rxn} during cure of Chemflake

Total Heat of Reaction = 243.81 J/g

Time (hrs)	Delta H	dH/dH total	ln dH/dH(tot)
0	243.81	1.00	0
1	221.78	0.91	-0.09
2	198.17	0.81	-0.21
4	164.11	0.67	-0.40
8	102.30	0.42	-0.87
24	146.46	0.60	-0.51
48	103.20	0.42	-0.86

Table 4.9 Change in Barcol-Hardness of Chemflake Coupons during cure at room temperature

Time	Hardness No.
3 hr 15 min	35
3 hr 45 min	44
4 hr 15 min	48
5 hr 15 min	55
12 hr 15 min	71
24 hr	75
after postcure	86

Figure 4.34 Alpha plotted with FDEMS data of Chemflake during cure

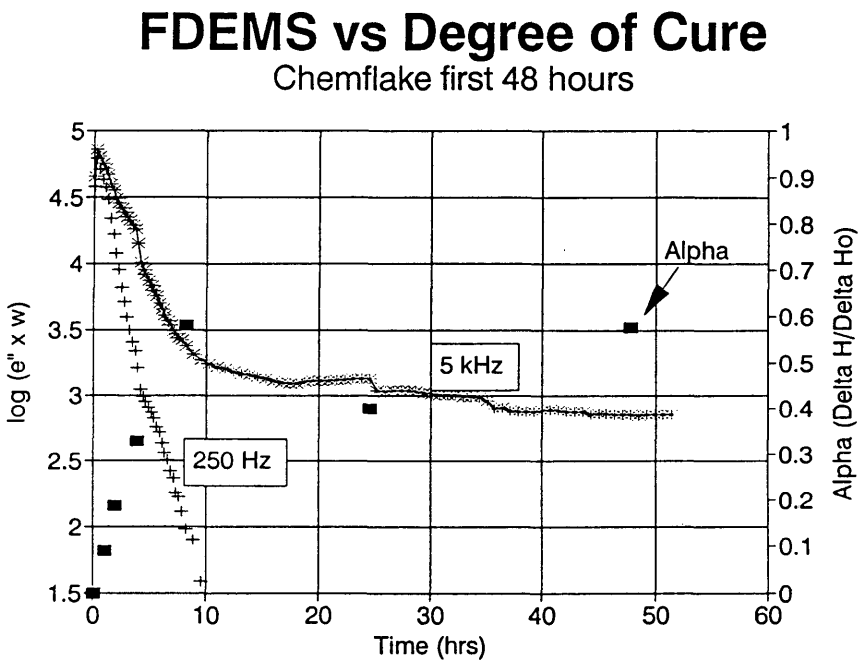

Figure 4.35 FDEMS vs. Alpha of Chemflake during cure

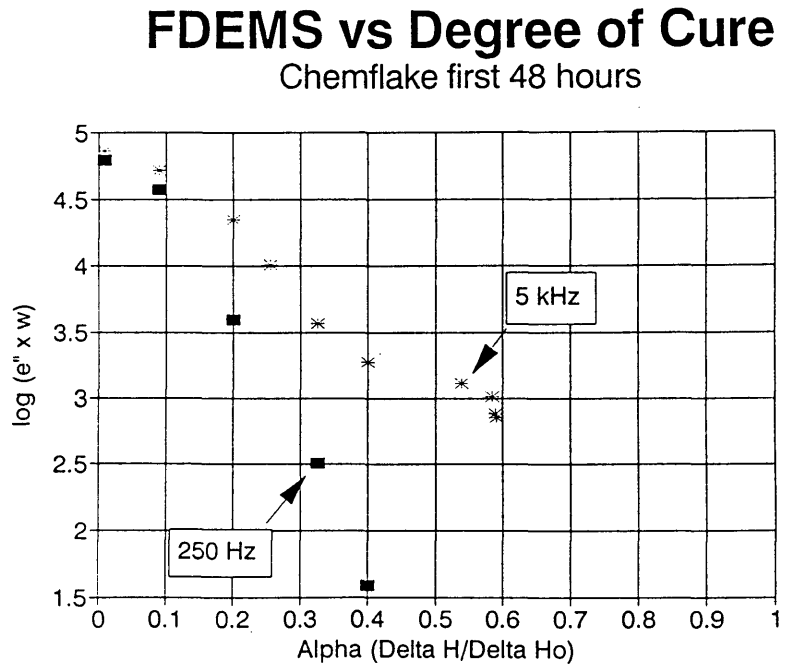

Figure 4.36 Barcol hardness plotted with FDEMS data of Chemflake during cure

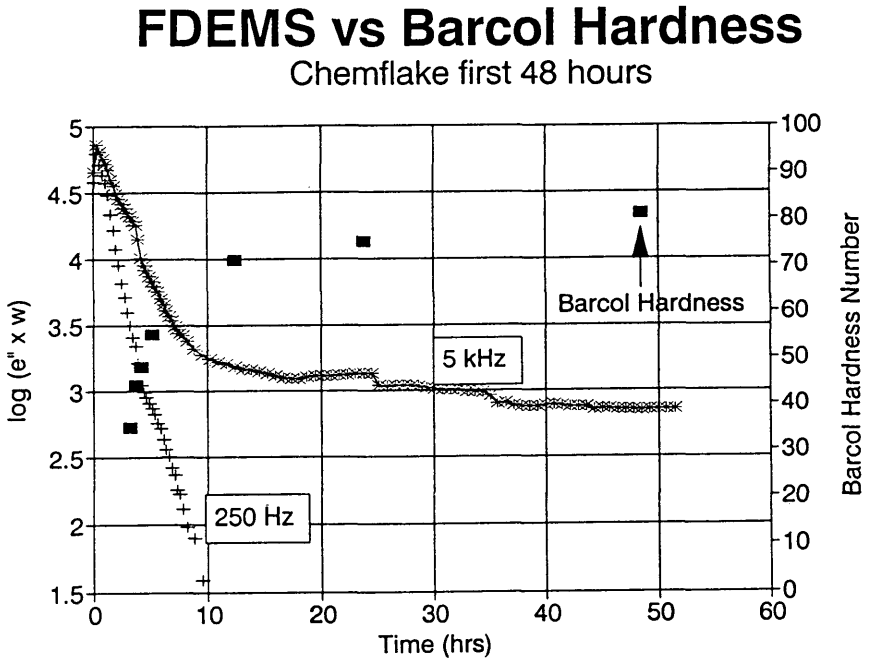

Figure 4.37 FDEMS vs. Hardness of Chemflake during cure

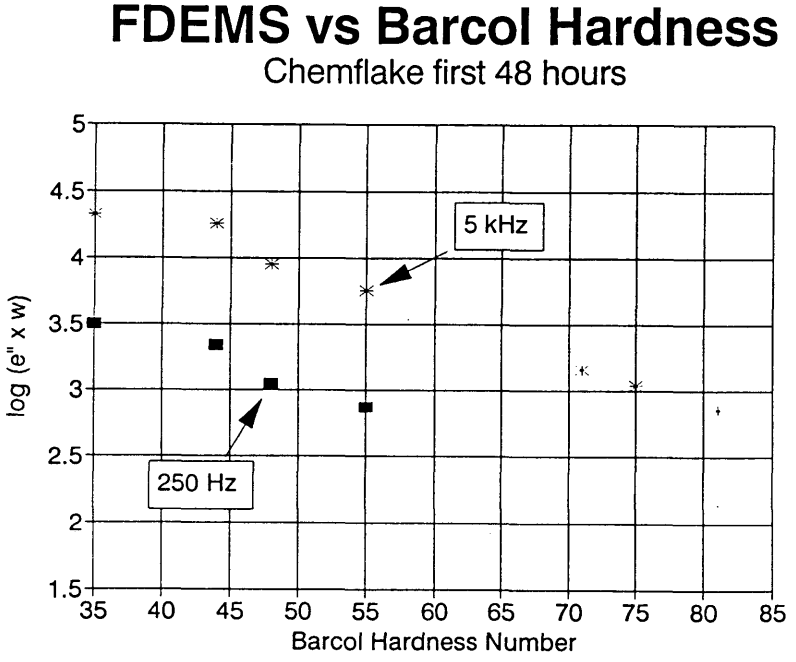

Figure 4.38 FDEMS of Chemflake in 45°C HCl, in vapor

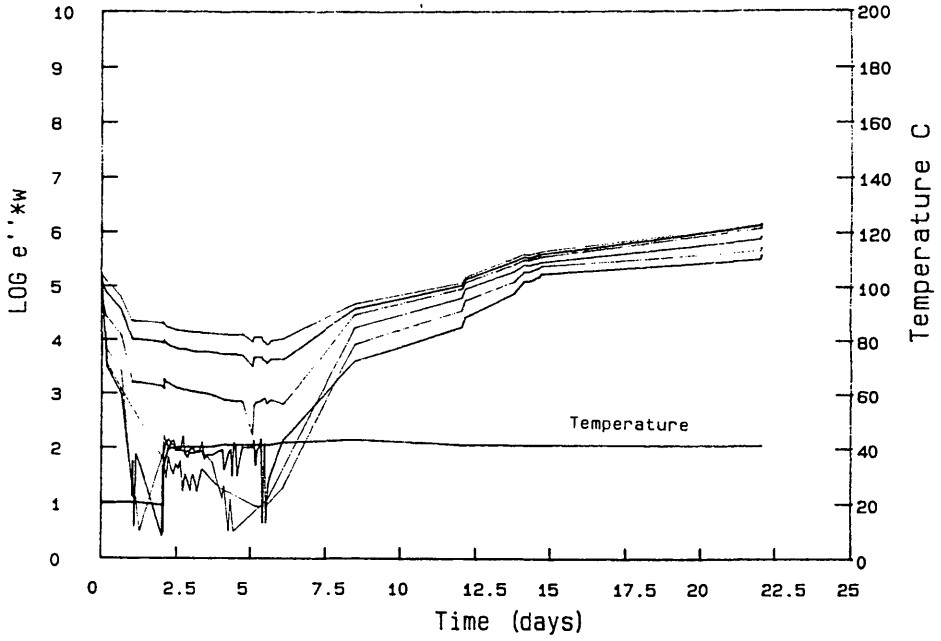

Figure 4.39 FDEMS of Chemflake in 45°C HCl, in liquid

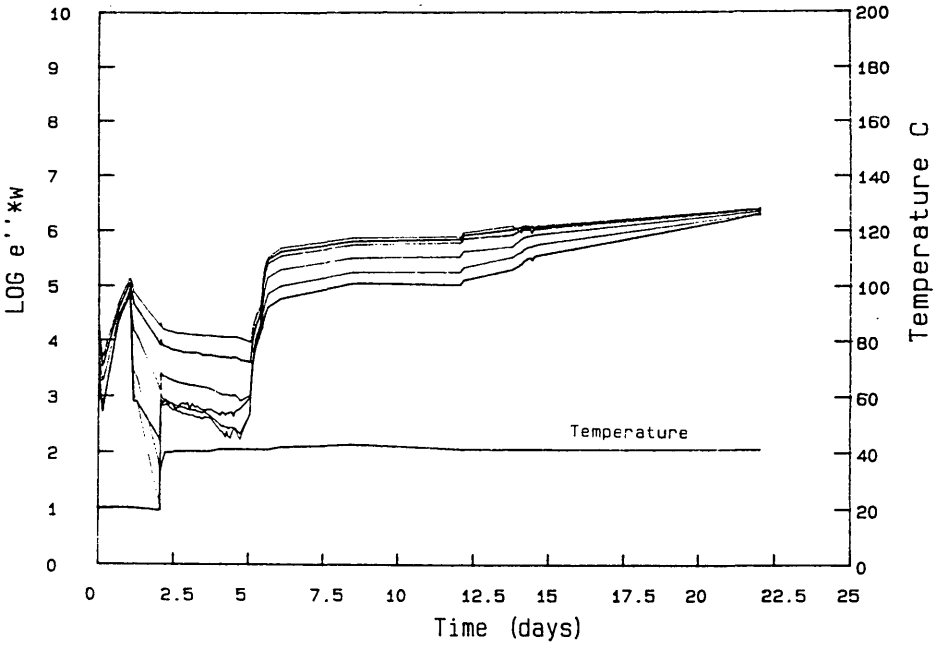

Table 4.10 Weight change of Chemflake coupons in 45°C HCl bath

Day	Mass				Mass Remaining			
	#1	#2	#3	#4	#1	#2	#3	#4
0	43.7224	42.2716	42.1191	41.8770	100	100	100	100
1	43.7328	42.2801	38.1893	38.0201	100.0238	100.0201	90.66979	90.78993
2	43.7501	42.2930	36.4848	35.3806	100.0634	100.0506	86.62293	84.48695
3	43.7731	42.3156	36.3411	35.3437	100.116	100.1041	86.28176	84.39883
7	43.8141	42.3610	35.0291	34.5693	100.2097	100.2115	83.16678	82.54961
10	43.8374	42.3866	34.6102	34.5053	100.263	100.2721	82.17222	82.39678
16	43.8685	42.4176	33.7169	33.4445	100.3342	100.3454	80.05133	79.86365
23	43.8967	42.4450	33.1064	32.8835	100.3987	100.4102	78.60187	78.52401
30	43.8956	42.4357	32.9446	32.6183	100.3961	100.3882	78.21772	77.89073
37	43.9128	42.3605	24.1283	32.4196	100.4355	100.2103	57.28589	77.41624
44	43.9450	42.4751	16.4812	25.8964	100.5091	100.4814	39.12999	61.8392

** #1 and #2 not immersed, but exposed to fumes **

Figure 4.40 Percent Weight remaining vs. Days of Chemflake coupons in 45°C HCl bath

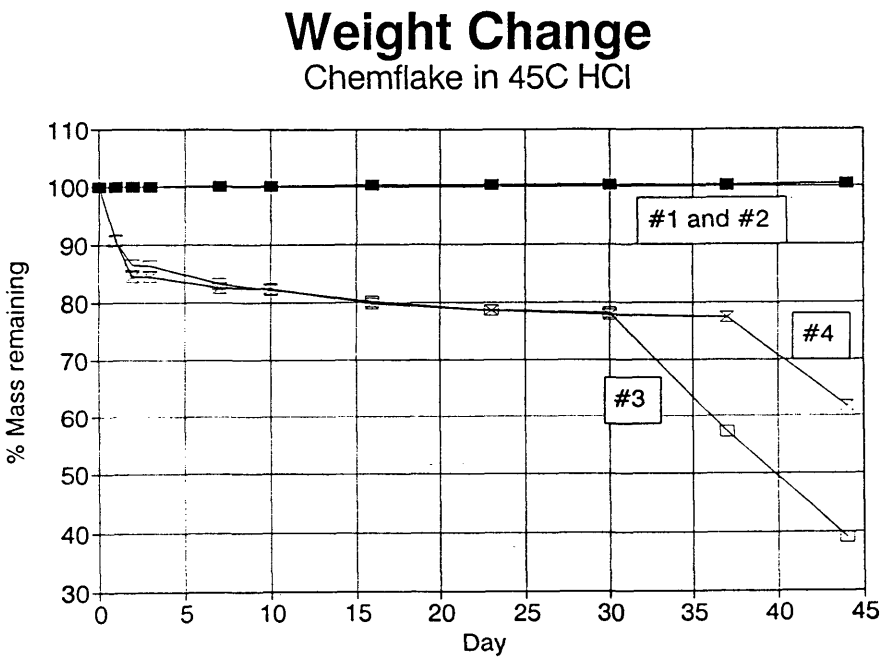

Figure 4.41 Barcol hardness vs. Days of Chemflake coupons in 45°C HCl bath

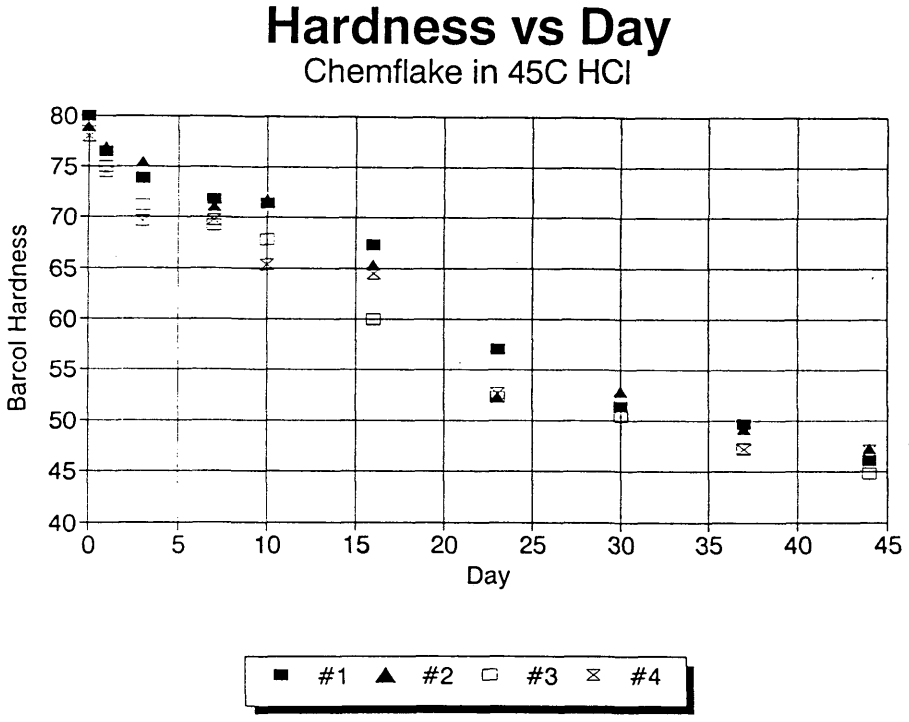

References for Chapter 4

1. McCullough, L. "Characterization of Nylon-11 Degradation," Master's Thesis, College of William and Mary, 1995.

2. Newbie, W. R. "*In Situ* Monitoring of Polymeric Degradation: Nylon-11 and PVDF," Honor's Thesis, College of William and Mary, 1996.

3. Hood, D. K. "Monitoring and Modeling of Infiltration, Polymerization, and Degradation Phenomena in Polymeric Systems," Ph.D Dissertation, College of William and Mary, 1996.

4. Veith, A. and W. Warrach. "Replacing ASTM D-471 Oils No. 2, No. 3". *Rubber and Plastics News*, Aug. 30, 1993.

Chapter 5. Conclusions

From the data gathered so far in the nylon study, it can be concluded that pH effect (at the level being tested) is not a significant factor on the rate of degradation of the polymer. Rather, the percent of water present in the environment surrounding Nylon-11 seems to determine the extent of molecular weight loss. The molecular weight calculated from samples in the 5% water sample is comparable to the molecular weight of samples from the 100% water, but both are much less than dry oil. Future studies may include even lower percentages of water, near 1%, to determine exactly where the level of degradation increases.

Preliminary studies of temperature effects in nylon show a direct correlation between the rate of degradation and temperature. The kinetic model presented will enable the prediction of molecular weight changes in different conditions.

The study involving PVDF has yielded several pieces

of information so far. Early data indicate that in air and 95% IRM oil/5% H_2O at high temperature (130°C), degradation of the polymer occurs slowly, as seen in the molecular weight data and the flat frequencies in the FDEMS sensor data output in these environments. This is important for the off-shore industry, which relies on PVDF to withstand continuous direct contact with oil at elevated temperatures.

Data from the PVDF in 100% Aniline and Ethylene glycol/10% Tetraethylammonium chloride show considerable amount of molecular weight loss. But normal operating conditions are in the range of less than 100 ppm for these compounds, so data at lower concentration levels must be examined prior to any conclusions being drawn.

The Chemflake study examines both the cure and degradation of the material. It is shown that the advancement of cure can be detected sensitively with both the DSC and FDEMS, as well as with hardness readings. The degradation of Chemflake in 45°C HCl was readily seen using FDEMS. It is speculated that the gold coated steel leads may have hastened the detected degradation, though the coupons seem to have withstood the concentrated acid with minimal penetration. Future studies in Chemflake

include the use of more acid-resistant wires along with the use of two thinner coats to seal up possible air voids within the material.

The use of FDEMS measurements has given an enormous advantage to polymer scientists. With this technology it is possible to examine microscopic behavior *in situ* within the material as it ages. There is still quite a bit to learn about polymeric systems; but with the ever increasing use of plastics and composites, new technology such as FDEMS along with older instrumentation such as the DSC and the viscometer will be able to decipher the aging processes of polymers during use in their operating environments.

Bibliography

Allcock, Harry R. and F. W. Lampe. Contemporary Polymer Chemistry. Englewood Cliffs: Prentice-Hall, Inc. 1990.

Chanda, Manas and R. K. Salil. Plastics Technology Handbook, 2nd edition. New York: Marcel Dekker, Inc. 1993.

Collier's Encyclopedia, 1987. Vol. 17.

Gruenwald, G. Plastics. New York: Hanser Publishers, 1993.

Hall, Christopher. Polymer Materials. 2nd edition. New York: John Wiley & Sons, 1989.

Hood, D. K. "Monitoring and Modeling of Infiltration, Polymerization, and Degradation Phenomena in Polymeric Systems," Ph.D Dissertation, College of William and Mary, 1996.

Inoue, M. "Studies on Crystallization of High Polymers by Differential Thermal Analysis." Journal of Polymer Science, Part A. New York: John Wiley & Sons, Inc., 1963.

Jahnsen, Thor H. Summary of Long-Term Testing of Chemflake; Porsgrunn, Norway, 1993.

Kalman, M. D., J. Belcher, and J. Plaia. "Advanced Materials for Flexible Pipe Construction." PD-Vol 53, *Offshore and Arctic Operations*, 1995.

Kranbuehl, D., D. Hood, L. McCullough, H. Aandahl, N. Haralampus, and W. Newby. "Frequency Dependent Electromagnetic Sensing (FDEMS) for Life Monitoring of Polymers in Structural Composites During Use." 1995, in press.

Lovell, Peter A. "Dilute Solution Viscometry". ***Comprehensive Polymer Science, Volume 1.*** New York: Pergamon Press. 1989.

Mark, Herman F. *et al.* Encyclopedia of Polymer Science and Engineering. 2nd edition. New York: John Wiley & Sons, 1989. Vol. 17.

McCullough, L. "Characterization of Nylon-11 Degradation," Master's Thesis, College of William and Mary, 1995.

McNaughton, J. L. and C. T. Mortimer. Differential Scanning Calorimetry. Reprint from "IRS; Physical Chemistry Series 2, 1975, Volume 10". London: Butterworths.

Newbie, W. R. "*In Situ* Monitoring of Polymeric Degradation: Nylon-11 and PVDF," Honors Thesis, College of William and Mary, 1996.

Nguyen, T. Degradation of Poly(vinyl Fluoride) and Poly(vinylidene Fluoride). JMS-Rev. Macromol. Chem. Phys., 1985. C25(2).

Seymour, Raymond B. Polymers for Engineering Applications. ASM International, 1987.

Smith, William F. Foundations of Materials Science and Engineering, 2nd edition. New York: McGraw-Hill, Inc., 1993.

Sperling, L. H. Introduction to Physical Polymer Science. New York: John Wiley & Sons, Inc. 1992.

Tipler, Paul A. Physics. New York: Worth Publishers. 1991.

Van Krevelen, D. W. Properties of Polymers. 2nd edition. New York: Elsevier Scientific Publishing Company, 1976.

Veith, A. and W. Warrach. "Replacing ASTM D-471 Oils No. 2, No. 3". *Rubber and Plastics News*, Aug. 30, 1993.

von Hippel, Arthur. Dielectric Materials and Applications. Cambridge: The M.I.T. Press. 1954.

Welch, Gordon, and Robert Miller. Journal of Polymer Science, Polymer Physics Edition. **Vol. 14.**

VITA

John Chen Yang

Born in Taiwan, January 5, 1973. Graduated from Manchester High School in Chesterfield, Virginia, June 1991. B.S. in Chemistry, the College of William and Mary, May 1995. M.A. candidate in Chemistry, the College of William and Mary, December 1996.

Upon graduation, the author plans on attending the University of North Carolina at Chapel Hill to pursue a Doctorate in Chemistry.